DEGREE PROJECT

Numerical Approach to the Design and Optimisation of a Bi-Propellant Pintle Injector

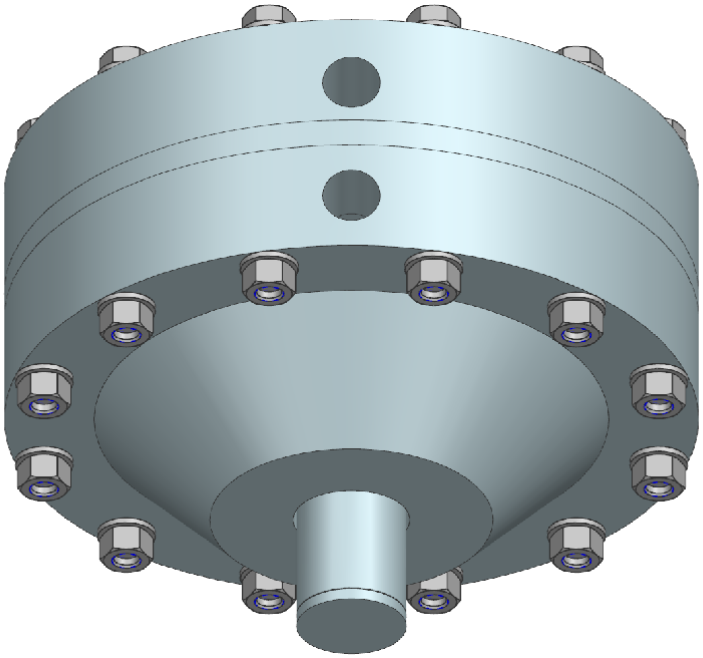

Erik Andersson

Space Engineering, master's level
2022

Luleå University of Technology
Department of Computer Science, Electrical and Space Engineering

LULEÅ UNIVERSITY OF TECHNOLOGY

Master Thesis

Numerical Approach to the Design and Optimisation of a Bi-Propellant Pintle Injector

Author:
Erik Andersson

Supervisors:
Dr. Alexis Bohlin
Dr. Jihyoung Cha

Examiner:
Prof. René Laufer

A thesis submitted in partial fulfilment of the requirements for the degree of Master in Space Engineering

in the

Department of Computer Science, Electrical and Space Engineering

December 5, 2022

Abstract

Rocket propulsion is of vital importance for space travel. New innovations are continuously developed in order to facilitate the demand of the rapidly evolving space sector. Recently a focus on reusable rockets has appeared due to the economical and environmental benefits they bring. When designing reusable launch vehicles the propellant injector becomes very important since it is a critical component when throttleabilty is desired. Which is a key element of landable rockets. Selecting an appropriate injector type therefore becomes crucial, a common injector type used for throttleable rockets is the pintle injector.

Unfortunately the design process of the pintle injector is complicated due to the large amount of variables that must be determined. This thesis aims to solve this problem by developing a numerical method to design and optimise a pintle injector and then produce a preliminary design.

The numerical method developed in this thesis is used to produce a preliminary design of a pintle injector designed to utilise a combination of liquid oxygen and gaseous methane, theoretically capable of a max thrust of 1000N and a throttleabilty of 5 to 1. The design had a focus on optimising the performance of the parameters sauter mean diameter, vaporisation distance and spray angle for the injector. The resulting injector showcases great performance and is deemed to show a successful preliminary design. Which shows that the numerical design and optimisation process that was developed also was successful.

Acknowledgements

I would first like to thank Dr. Alexis Bohlin who first introduced me to this thesis project, I have enjoyed the subject and have learned a lot during this time. I would also like to express my gratitude to Dr Jihyoung Cha who has helped me throughout the project, his advice and assistance cannot be underestimated.

Finally, to my friends, fellow students and family, thank you for keeping me sane these past five years. This journey would have been much harder without you.

List of Abbreviations

CEA	Chemical Equilibrium and Applications
LOX	Liquid oxygen
LRE	Liquid-propellant Rocket Engine
NTO	Nitrogen Tetroxid
OF	Oxidiser to fuel
PWM	Pulse Width Modulation
SMD	Sauter mean diameter
TMR	Total momentum ratio

List of Symbols

A	Area
B	Transfer number for droplet vaporisation
c^*	Characteristic velocity
C_d	Discharge coefficient
C_F	Thrust coefficient
c_p	Specific heat ratio
D	Diameter
D_{32}	Sauter mean diameter
F	Thrust
h_{fg}	Latent heat of vaporisation
J	Cost
k	Thermal conductivity
L	Length
$\dot{m}$	mass flow
p	Pressure
Pr	Prandtl number
Q_{level}	Thrust level weighting
Q_D	SMD weighting
Q_α	Spray angle weighting
Q_X	Vaporisation distance weighting
q	Variable for SMD correlation
r	Radius
R	Gas constant
T	Temperature
U	Velocity
We	Weber number
X	Vaporisation distance
α	Spray angle
δ	Thickness
γ	Specific heat ratio
Γ	Variable for droplet vaporisation
ε	nozzle expansion ratio
θ_{pt}	Pintle tip angle
φ	Drag coefficient for vaporisation model
ξ	nondimensional pintle tip angle
ρ	Density
σ	Surface tension

Subscripts

a	Ambient
ann	Annular orifice
c	Combustion chamber/combustion gas
$d0$	Initial droplet condition
e	Nozzle exit
f	Fuel
o	Oxidiser
pt	Pintle tip
$sleeve$	Pintle sleeve
t	Nozzle throat
tot	Total

Contents

List of Figures

List of Tables

CHAPTER 1

Introduction

Rocket propulsion is of vital importance for space travel and for launching satellites into orbits around the earth. The field of rocket propulsion is vast and consists of many disciplines that come together into a fine engineering art. Today, there is a rapidly expanding field of launch providers and as they strive to reduce launch costs a focus on reusable rockets has appeared. The economical benefits of reusable launch vehicles are great, the cost of reusing a vehicle is significantly lower than constructing a brand new one for each launch mission. Reusing launch vehicles will also reduce the overall environmental impact of rocket projects. The reusability of vehicles in use today varies, where only a handful of vehicles can boast that they are nearly completely reusable. When designing a reusable vehicle the main challenge is finding a way to safely return the vehicle to ground. One way this can be accomplished is by using the rocket engine of the vehicle to safely descend and land. Using the engine to land means that the engine must be able to control its thrust, without thrust control the vehicle will be unable to accurately control its descent. Thrust control in propulsion systems can take many forms. But in the case of propulsive landing, controlling the flow of propellants into a liquid-propellant rocket engine (LRE) is by far the best option. The process of controlling the propellant flow is called throttling [1][2].

The propellant injector of the engine comes into focus when designing a throttleable rocket engine. Since the injector is responsible for controlling the flow of propellants into the thrust chamber it becomes the main way to achieve throttling. The injector also ensures that fuel and oxidiser are distributed and mixed properly in the combustion chamber in order to facilitate the most optimal combustion process. There are few components in a LRE as important as

the propellant injector, the design of the propellant injector is critical and can mean the difference between an excellent rocket and total failure. There are several types of injector designs and by selecting the appropriate type one can significantly improve the performance of the rocket engine [1][2].

The pintle injector is a highly suitable candidate when designing throttleable rockets due to its potential for very high performance and high degree of throttleabilty, it is highly suited for applications such as landers. The pintle injector will also minimise combustion instabilities in the chamber and increase the mixing potential of bi-propellant engines. While the advantages of the pintle injector are great they are difficult to design due to the large amount of variables that must be determined in order to reach a completed design. It is therefore important to limit scope of the design process to only include the most important parameters [3].

For many reasons, such as a competitive marketplace, an engineer might not only be interested in a design which works at some sort of nominal level, but is the best design in some way. The process of determining the best design is called optimisation. In order to find the optimal design the design is usually formulated into some type of optimisation problem that must be solved. There are multiple ways to solve an optimisation problem, where using a computer aided numerical approach is highly suited for complex systems with multiple variables [4].

1.1 Project Motivation

Unfortunately information regarding the pintle injector is limited, most research on the injector is done internally by companies or agencies and the results are rarely disclosed. This is further complicated due to the fact that modelling combustion processes can be very difficult and in the case of injector performance for rocket engines the task becomes practically impossible to accurately model [5]. What this means is that practical testing is almost always required if one wishes to develop propellant injectors. Being dependant of practical testing in a design process is highly disadvantageous, as this will significantly increase cost and time. Therefore there exists a need to develop a process where an injector can be designed and optimised without relying on practical testing.

1.2 Objective

The objective of this master thesis is to produce a method of applying numerical relationships to design and optimise a pintle injector. In order to simplify this process the design will focus on the outlet region of the injector. This method will then be applied in order to produce an example of a preliminary design. The example design will be of small scale and there shall be a focus on maximising

performance. The method itself shall also be able to be applied to a variety of projects, and should therefore be easily adaptable and changeable based on individual hypothetical project demands.

1.3 Thesis Outline

2 Literature Review
This section presents the general injector operation and how throttling can be achieved. The pintle injector is also described in detail with some notes on propellant selection and cold flow testing.

3 Theoretical Background
In this section the underlying equations used in the thesis are presented.

4 Initial Conditions
Here the initial conditions of the injector are described, these include requirements that will impact the design process of the injector outlet region. This section also contains the process used to find the required propellant mass flows.

5 Design Process
In this section the numerical approach is applied to the design process. Here the design process that was developed is described and applied.

6 Discussion
Here the injector that was acquired from the design process is evolved into a full injector design. Simulations are performed in order to validate the theoretical performance of the injector.

7 Conclusion
This last section of the report concludes the project and provides notes on future work.

CHAPTER 2

Literature Review

2.1 The Injector

The injector has to introduce and meter the flow of propellants to the combustion chamber, cause liquids to be broken up into small droplets (a process called atomisation), and distribute and mix the propellants in such a manner that a correctly proportioned mixture of fuel and oxidiser will result, with uniform propellant mass flow and composition over the chamber cross section. In order to evaluate the combustion performance of an injector the term characteristic velocity (c^*) is often used, it can easily be measured in hot fire tests and then be compared to theoretical calculations. The ratio between these numbers is then considered to be the combustion efficiency. Characteristic velocity can be acquired through equation 3.5. c^* is independent of nozzle characteristics which makes it ideal for evaluating both injector performance and propellant properties [1].

Ensuring optimal combustion performance is vital for the overall performance of the engine, each percentage point lost in combustion efficiency results in a loss of the same magnitude in overall propulsive efficiency. Well designed injectors can reach efficiencies so close to 100% that the ability to measure the parameter is the limiting factor in its determination. The space shuttle main engine RS-25, for instance, exhibited a combustion efficiency of 99.7%. Depending on the specific application efficiencies that fall below 90% can also be considered acceptable and is determined by the specific mission requirements [6].

While there are several possible injector design types most injectors follow a simple principle of colliding the fuel and oxidiser fluid flows into each other.

This causes liquid propellant to start to break up into droplets and to mix with the second propellant. The point where the propellants meet is called the impingement point.

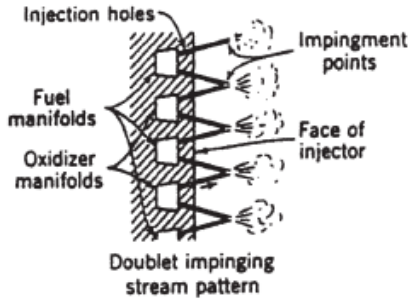

Figure 2.1: Illustration of a basic bi-propellant injector. The impingement points and how they are produced from the collision of the propellant streams are of special interest [1].

One of the more basic injector designs will use a plate with multiple holes arranged in a sort of shower head style pattern. This type of injector is quite easy to design and can easily be scaled up or down depending on the application demands. This design is usually referred to as a showerhead injector and is a type of fixed geometry injector [1].

2.2 Throttling

The term throttling is most often used to describe a varying thrust profile or thrust modulation in a rocket engine. This nomenclature is used because one of the most common methods of thrust control for LREs is to regulate the propellant flow rates by control valves. The possible applications of throttleable LREs are almost endless and each have different demands on the throttleability of the engine [3].

The throttleability is usually expressed as a ratio between the maximum and minimum thrust levels that the engine is capable of, for instance an engine with a max thrust of 40kN and a minimum thrust of 5KN would have a throttleability of 8-to-1. The throttleability requirements of different engines can vary greatly and if a project requires 5-to-1 or higher throttleability it is said to require deep throttleabilty. Throttling demands can range from as low as almost 1-to-1 to as high as 100-to-1 for ballistic missiles and orbital rendezvous, where more precise orbital control may require even higher ranges. This is a very high throttleabilty range and most applications do not require such a degree of throttleability [3][7]. The most commonly used methods for throttling are briefly described below.

High Pressure Drop Injectors
A typical LRE with a single, fixed-geometry injector can generally be throttled approximately 2-to-1 or 3-to-1. It throttles by increasing or decreasing the pressure feeding the propellant, this means the flow will also be increased or decreased. However this presents risk to the system since lower pressures can cause instabilities in the upstream flow. This means the injector and feed system must operate at higher than usual injector pressure drops for higher thrust levels in order to maintain an acceptable pressure drop at minimum thrust if deep throttling is required. The main advantage of this type of throttling is its simplicity, the main disadvantage is the high pressure requirement it imposes on the whole system [3].

Dual-Manifold Injectors
A dual manifold injector essentially combines two fixed geometry injectors with independent feed systems to achieve higher degrees of throttleabilty. Deep throttling is achieved by using two-manifold operation at high thrust and single-manifold at low thrust, essentially changing the effective injection area. this operation can be as simple as closing a valve. The transition between two- and single-manifold operation can be quite abrupt and the injector must be properly designed in order to enable a smooth transition [3].

Gas Injection
Gas injection is a throttling method that introduces a much lower density fluid into the propellant flow. This reduces the bulk density of the propellants which will reduce the total mass flow through the engine. This can be quite a dangerous operation and extra care has to be taken to ensure smooth injection of the added fluid. There are reports of this method causing high frequency pressure fluctuations in the propellant feed system which can carry significant risk [3].

Multiple Chambers
In this concept one engine consists of several small thrust chambers which can be independently operated, thus the thrust can be modified by throttling multiple chambers by a small amount. This system does however add significant complexity and weight [3].

Pulse-Width Modulation (PWM)
By rapidly turning an engine on and off a quasi-steady state of average thrust can be acquired. PWM engines usually suffer from low performance and require fast response feeding systems and are thus mostly used where small and rapid thrust corrections are needed, such as in satellite rendezvous [3].

Throat Throttling
By changing the throat area the propellant flow will be blocked and the chamber pressure will increase. With a constant propellant pressure this increase in chamber pressure will cause a decrease in the injection pressure drop and

thus a decrease in propellant flow. The main concern when designing a throat throttled engine is that the blocking mechanism will be subject to high thermal and structural loads and that it requires a high pressure propellant feed system due to the higher chamber pressures at low thrust [3].

Hydrodynamically Dissipative Injector
This injector type uses fluid dynamics to create resistance across the injector. This can be accomplished by capillary tubes that create high pressure drops due to viscous losses or long element features to create added fluid mass or inertance as additional impedance. This method is quite limited in throttling range [3].

Variable Area Injector
By changing the area of the injection orifice the pressure drop across the injector can be maintained for a wide range of thrust levels. This is one of the better options when designing engines with deep throttling requirements and solve a lot of the inherent disadvantages of other options. A variable area injector won't require an excessively high pressure feed system or extra propellant additives. The only major disadvantage is some added complexity in the actuating elements [3].

2.3 The Pintle Injector

The pintle injector is a type of variable area injector. It is one of the most commonly used types of variable area injector due to its relatively simple design. The basic concept of a pintle injector is shown in figure 2.2.

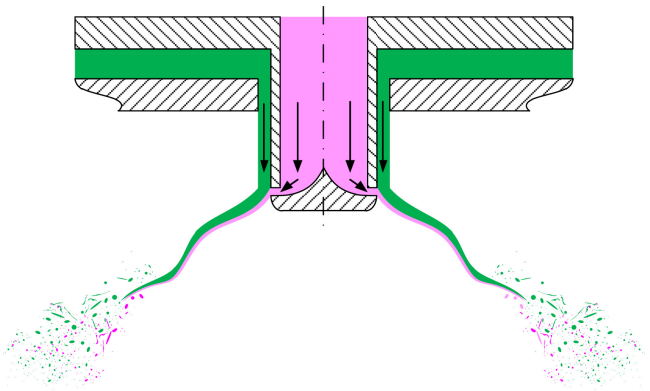

Figure 2.2: Cross section of the basic pintle injector concept. The path of the propellant though and out of the injector are of importance [8].

One propellant (shown as green in figure 2.2) is fed through the outer flow passages into a circumferential annulus and out into the combustion chamber. This

propellant exits the injector through what will be referred to as the annular orifice as an axially flowing annular sheet and arrives at the impingement point with a circumferentially uniform velocity profile. The other propellant (shown in figure 2.2 as pink) enters via a separate central passage and flows axially towards the pintle tip. As it hits the pintle tip it is turned into a radially uniform flow and directed towards the impingement point. This propellant exits through what will be referred to as the pintle gap. The variable area comes through the control of the position of the pintle tip. By moving the pintle tip up or down the exit area of the pink propellant can be changed. This method of area control is advantageous since it is quite simple to actuate it, a simple linear mechanism can be employed without much difficulty. This also gives the pintle injector far greater throttleability than most injector types as the potential orifice area of the injector can have a significant range. Pintle injectors can easily achieve throttling ranges that far exceed deep throttling demands while also ensuring combustion efficiency. For instance, the MIRA 5000 engine was capable of throttling 35 to 1 while utilising a single pintle injector element and reported performance in excess over 93% of theoretical c^* [9].

An example of an actual pintle injector can be seen in figure 2.3.

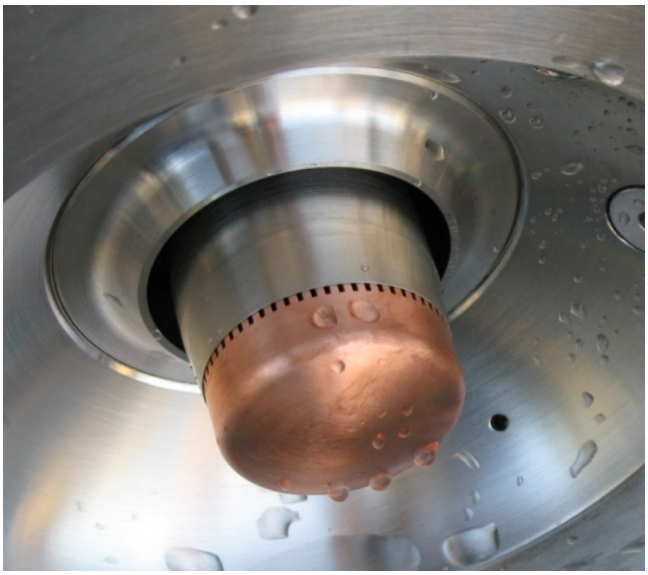

Figure 2.3: Example of a complete pintle injector. The large gap around the central cylinder is the annular orifice, the small holes near the tip of the pintle is the pintle gap. In this report this gap will be one continuous gap around the entire pintle [10].

A more detailed schematic of the pintle injector outlet region can be seen in figure 2.4.

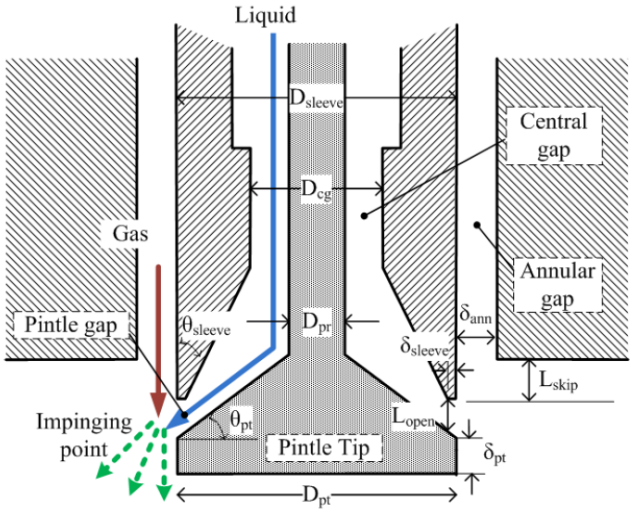

Figure 2.4: Schematic of the outlet region of the pintle injector, the various measurements in this figure will be referred to as design variables. Pintle tip angle θ_{pt}, pintle tip diameter D_{pt}, opening distance L_{open} and annular gap thickness δ_{ann} will be of special interest [11].

Figure 2.4 illustrates the main challenge when designing pintle injectors. There is a great number of design variables and one must identify which ones are important to the design process in order to not become overwhelmed [3]. The flows out of the outlet region will combine and form a spray, illustrated in figure 2.5.

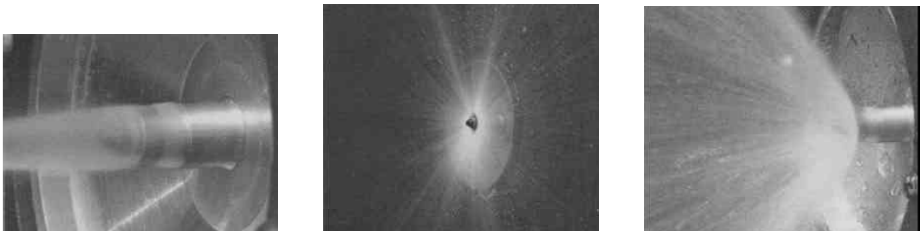

(a) Annular flow only *(b) Pintle flow only* *(c) Combined flows*

Figure 2.5: Examples of flow through each orifice, showing the flow directions of each propellant [9].

The combination of these flows will form a conical spray with an angle alpha according to figure 2.6.

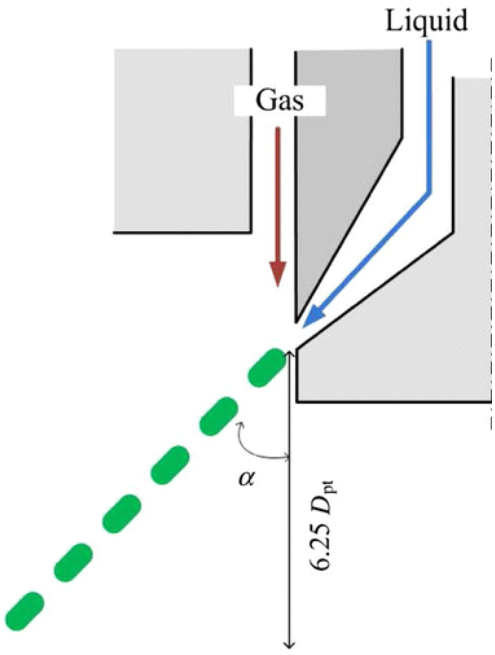

Figure 2.6: Illustration of the pintle spray angle. The green dashed line represents the combined propellant flow, note the position of the spray angle α [11].

This spray is one of the primary advantages of the pintle injector. The spray can quite easily cover the entire cross section of the combustion chamber. As long as the mass flows out of the injector is uniform the propellant distribution will also be uniform while only using a single injector element. Traditional injectors are thus often much bigger and heavier than comparable pintle injectors. The conical spray may also produce a beneficial flow within the combustion chamber called recirculation zones. As the spray angle increases to above roughly 20° two recirculation zones may appear. The first is the core recirculation zone, this is a torus shape around the central axis of the combustion chamber within the conical spray. The second is the mantle recirculation zone, this is a torus shape around the central axis positioned between the chamber walls and the outer surface of the spray. Figure 2.7 shows an illustration of the flow patterns in a combustion chamber using a pintle injector [9][12].

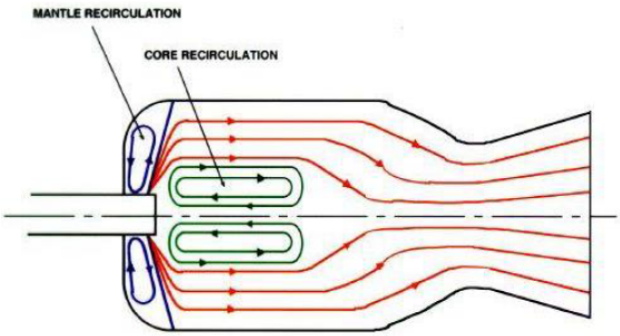

Figure 2.7: Axial cross section of chamber flow patterns in a LPR using a pintle injector [11].

Both recirculation zones are beneficial to overall engine performance but have different functions. The core recirculation zone is the main area where combustion will occur. It is often desirable to maximise the size of this zone in order to ensure uniform combustion throughout the chamber. The mantle recirculation zone will mostly consist of unburnt propellant and its main benefit is the cooling effect it will have on the top of the chamber. Both zones will also significantly improve the mixing of propellants in the chamber [13].
The recirculation zones will also eliminate the risk of acoustic instability within the chamber. Acoustic instability is essentially the propagation of acoustic waves in the combustion chamber. These waves can generate strong pressure waves that will impact combustion efficiency and may damage the chamber [14]. Traditional showerhead-style injectors will produce an axially flowing uniform flow field and combustion mostly occurs on a flat plane parallel to the injector face. This flow field makes this chamber vulnerable to acoustic instability and the chamber must therefore be designed to hinder the formation and propagation of acoustic waves. This is usually done with the addition of baffles and cavities, something that is almost unnecessary for chambers designed for pintle injectors. According to TRW, the original inventors of the pintle injector, there has never been a case of acoustic instability in their pintle injector engines [9].
In order for the chamber to support the recirculation zones the chamber has to both be longer in physical length and higher in contraction ratio. This means pintle injector engines are generally larger than comparable engines [9].

2.3.1 Fuel and Oxidiser Centred pintle

When designing the pintle injector a decision has to be made whether fuel or oxidiser is to be the central propellant. Previous experience has shown that both choices are valid and high performance can be acquired with both configurations. If fuel is selected as the central propellant the flow can be configured to provide fuel film cooling to the chamber walls, this is therefore a popular choice when

designing the injector. If this feature isn't desired the decision on the central propellant is usually taken based on the design of the surrounding systems [9].

2.3.2 Movable Pintle and Movable Sleeve

There are two options when deciding how to control the area of a pintle injector. Either the pintle is moved and the sleeve is fixed or the pintle is fixed and the sleeve is moved, seen in figure 2.8. The moving pintle and fixed sleeve is the most basic of these two options and the movable sleeve is considered to be a general improvement over the original moving pintle design. This is mainly due to the fact that the moving pintle design is unable to provide area control of the annular orifice, something the moving sleeve design is capable of [9][11].

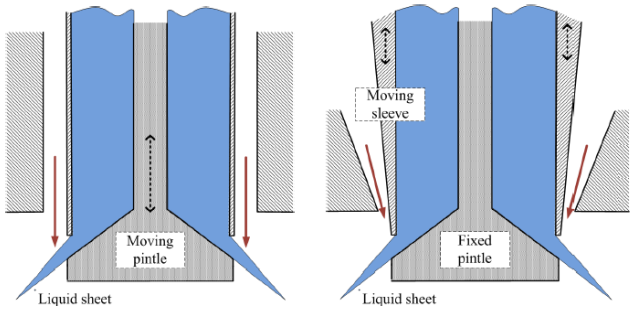

Figure 2.8: Illustration of the difference between moving pintle (left) and moving sleeve (right) design. Note that the increasing diameter of the moving sleeve will reduce the area of the annular orifice as it moves down [11].

The Moving sleeve does however have the disadvantage of adding increased complexity to the design. Mostly due to the difficulty of sealing a moving sleeve vs the relatively easy sealing of a moving pintle rod [9].

2.4 Atomisation

In order to measure the atomisation performance of the injector one must first select an appropriate way to represent the droplets of the spray. Since the injection process can't produce a spray in which all droplets are of a uniform size an appropriate representation of average droplet size has to be selected. There are several options for how to represent the average droplet size to evaluate, where Sauter mean diameter (SMD) is the most appropriate one for this thesis. SMD will describe the average droplet size in the form of a droplet diameter, where the ratio between the droplets surface area and volume is equal to that of the entire spray [15]. SMD is the most appropriate representation since combustion can only occur on the surface of a droplet. Therefore the surface to volume ratio is of particular interest for combustion processes and the SMD

will give info on this for the entire spray through just one number [5].
The atomisation performance can then easily be evaluated by simply checking the diameter, where smaller diameters indicate better atomisation performance.

2.5 Mixing

Evaluating the injector mixing performance poses a challenge in the preliminary design process. The mixing quality is dependant on the fluid flow out of the injector and the best way to evaluate it is through CFD simulation on a design candidate, which makes it difficult to design with mixing quality in mind since a lot of engineering hours have to be spent before mixing quality can be properly evaluated. However there are a couple of guidelines that can be applied in order to optimise mixing performance in the early stages of the design process.
The first is to ensure a uniform distribution of the propellants in the thrust chamber, the pintle injector itself will provide good distribution due to the spray that it naturally produces. By ensuring that the mass flow out of the injection orifices is as uniform as possible the spray will also have a uniform distribution of propellant [1].
Another goal of the design should be to ensure that recirculation zones can form in the thrust chamber. Recirculation zones are a priority since the circular flow in these zones is very beneficial for mixing. It has been shown that larger spray angles will increase the size of the central recirculation zone and increase overall combustion performance [9][13].

2.6 Propellants

Selecting the proper fuel and oxidiser combination is an important step in any rocket project, the chosen combination will influence every part of the design by governing the mass flow through the engine that will provide the desired thrust. There are many candidates to chose from when selecting a propellant combination and usually a comprehensive trade-off study has to be conducted in order to find the optimal combination for the specific design [6]. Conducting such a trade-off is outside the scope of this project, however a limited version of this trade-off study has been performed. The main goal is to find a propellant combination that can be safely handled, is relatively cheap and has research potential. A few candidates are briefly described here.

2.6.1 Oxidiser

Liquid oxygen (LOX)
One of the most commonly used oxidisers is liquid oxygen (LOX), it provides high performance for a large variety of fuels while also being chemically stable and noncorrosive. It does provide some challenge because of its low boiling point

of about 90K which makes pumping, valving and sealing extra difficult. The low boiling point also makes it harmful when in contact with human skin as it can cause severe frostbite. Spontaneous combustion with organic compounds is uncommon at ambient pressures, however there is a risk of combustion and explosions when a confined mixture is suddenly pressurised [1].

Nitric acid (HNO_3)
Nitric acid is highly corrosive. Only certain types materials including gold and a few variants of stainless steels are able to be used as storage and tubing. However with a small addition of flouride ion the corrosive effects on materials can be reduced, this mix is called inhibited red fuming nitric acid. The inhibitor does however increase the risk of blockages in valves and injector orifices. vapours from nitric acid are toxic and exposure limits must be considered when handling it. Droplets can cause burns and sores on skin contact. Nitric acid has been used with gasoline, amines, hydrazine and alcohols. It is hypergolic with hydrazine, furfuryl alcohol, aniline and other amines [1].

Nitrogen tetroxid (N_2O_4) or (NTO)
Most commonly used with hydrazine and its derivatives, the biggest advantage of NTO is its ability to be easily stored. It can be stored indefinitely in sealed containers made of appropriate materials and is the most common storable oxidiser in use today. NTO does however present several safety concerns. In its pure form is only mildly corrosive but will form strong acids when exposed to water, and can absorb moisture from the air. Additionally NTO fumes are highly toxic. It is also hypergolic with many fuels and can spontaneously ignite when it comes in contact with many common materials such as wood, paper and grease [1].

2.6.2 Fuel

Liquid hydrogen (H_2)
Liquid hydrogen is a cryogenic fuel with a boiling point of about 20K, the coldest of all known fuels. This low temperature makes handling and storing of liquid hydrogen very challenging, however its excellent performance makes it a very attractive fuel if one can deal with the difficulties of cryogenics. Liquid hydrogen is both non-toxic and non-corrosive, its combustion products are also often non-toxic depending on which oxidiser it has been paired with. The greatest danger when handling hydrogen is its flammability, hydrogen gas and air is explosive over a wide range of mixture ratios. Extra care must therefore be taken to make sure that escaping excess hydrogen gas does not pose a risk. Liquid Hydrogen has been used to great success in a wide range of space launch systems and is a very popular choice when designing high performance rockets [1].

Ethanol (C_2H_5OH)
Ethanol has a history in rocketry, it was widely used for early rockets but was

eventually mostly abandoned when higher performance fuels such as kerosene were discovered. Today Ethanol is mostly used by amateur and student projects or where performance isn't of great concern. Ethanol is relatively safe to handle, quite cheap and easy to acquire. The combustion products are also often non-toxic further simplifying the handling of it as a fuel [16].

Methane (CH_4)
Methane has for several decades been considered an attractive rocket propellant, but most efforts have been focused on more traditional fuels [17]. Recently this trend has been broken and several engines using methane are being developed, with one of the more high profile examples being SpaceX's Raptor engine [18]. One of the main advantages of methane is the clean burn it provides, many fuels will produce soot and other impurities that may contaminate surfaces exposed to its combustion. When designing reusable rockets this causes many problems and must be cleaned, by using methane the need for cleaning can be minimised and rockets can be refurbished and reflown much quicker [17][19]. Methane in its liquid form is a cryogenic fuel with a boiling point of about 110K. Quite close to that of LOX, it therefore presents many of the same challenges as LOX. Methane also presents exciting possibilities as a potential fuel for martian missions due to its ability to be produced locally on mars with in-situ fuel production [20].

2.7 Cold Flow Testing

Cold flow testing is a critical part in the development of rocket engines and one of the first practical tests that injectors undergo. Cold flow testing can take many forms and is a general term for anytime a fluid flow is used in testing without combustion. The main goal of cold flow testing is to investigate the flow behaviour within and out of the injector, the most basic type of cold flow test usually replaces the propellants with water and air. While water and air aren't the best analogues for the fuel and oxidiser important parameters such as flow resistance, spray pattern and visual observation of flow streams can be investigated. Flow resistance tests are required in order to accurately calibrate inlet pressures, it can also be used to evaluate manufacturing quality. Visual observation can complement this data by identifying potential orifice blockages or other design problems. Visual observation of the spray pattern can help in identifying impingement problems by checking the uniformity of the spray. The spray pattern can also give clues to the how the combustion process will interact with the thrust chamber wall [6][21].

It also possible to investigate the mixing performance by using two nonsoluble liquids as propellant analogues and then collecting the spray in a grid system. The mixing quality can then be evaluated by measuring the mass ratio at each position in the grid, these liquid/liquid mixing tests are easy to set up and relatively inexpensive. Gas/liquid mixing tests can be performed by measuring the gas velocity at each grid position instead of the collected mass. These tests are

more difficult to set up and are subject to a higher degree of error, but can still produce useful data [6][22].

One can also investigate the atomisation performance of the injector by measuring the droplet sizes in the spray, these tests are one of the most important tests that can be conducted in a cold flow setup. These droplet size measurements are typically performed by some form of laser instrument through for instance doppler interference, diffraction or other nonintrusive optical measurements. These techniques can suffer somewhat from an obscured view from high mass flow rate when investigating larger engines, but this shouldn't cause concern in this project due to the small scale of the engine [6].

2.8 Optimisation

Optimisation is a common problem in engineering where one often has to find the best possible solution to a problem where no objectively correct solution exists. This solution is found by changing variables that can be controlled, which are often subject to constraints. When dealing with simple systems this process can be accomplished through a combination of the engineers experience and judgement. This type of experience-based optimisation can fall short of identifying the optimum design, particularly when dealing with larger systems. The interactions of most practical problems are too complex and the variables too numerous to intuitively determine the optimal design. By using numerical approaches, together with optimisation algorithms, problems of increasing complexity can be solved.

Design optimisation is a tool that can replace an iterative design process to accelerate the design cycle and obtain better results. The design optimisation process can be represented using a flow diagram, such as the one in figure 2.9.

Figure 2.9 shows how a conventional design process can be changed by introducing an optimisation algorithm. The main disadvantage of the conventional process is the manual iteration loop. Using this method will be time consuming, and as discussed previously, highly impractical for complex systems. The evaluation of the design in the optimisation algorithm approach is strictly based on numerical values for the objective and constraints. The design changes are made automatically by the optimisation algorithm and do not require intervention from the designer. When a rigorous optimisation algorithm is used, the decision to finalise the design is made only when the current design satisfies the optimality conditions that ensure that no other design is better [4].

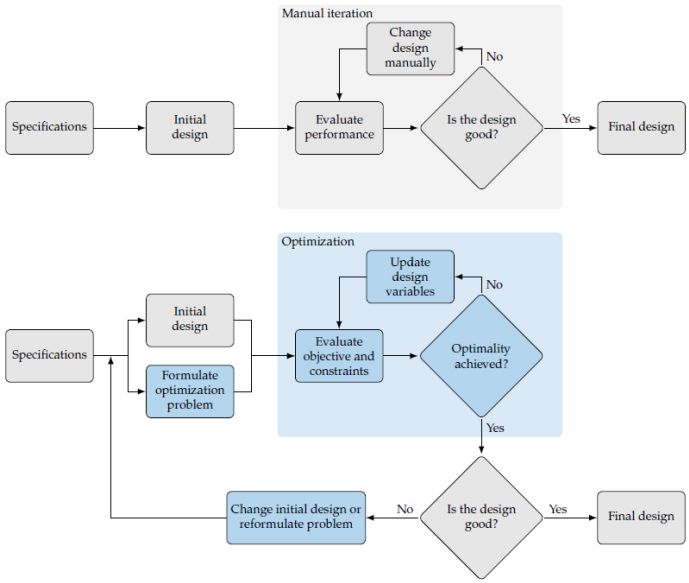

Figure 2.9: Conventional (top) versus optimisation algorithm process (bottom). By comparing these two charts the main additions of using a optimisation algorithm can be seen [4]

Since the optimisation algorithm results are completely dependant on how the algorithm was designed and how the optimisation problem was formulated there is a need to evaluate the results of the algorithm. This is done by the algorithm user through their own judgement. After this evaluation the initial conditions of the optimisation algorithm may be changed if necessary, the design may also be finalised if the results are satisfactory [4].

There are a multitude of options when selecting how to design the optimisation algorithm. For the design process in this project a quadratic optimisation method was chosen, this is done in the form of a quadratic cost function (seen in equation 3.23). This method was chosen due to to several reasons. The first is that this method produces optimisation problems that are generally more predictable and easier to solve, while guaranteeing that there is only one global minimum where the optimal solution is found. It is also highly appropriate when dealing with nonlinear systems, which this design process contains. The cost function used in this method can also easily be modified to fit a variety of applications [4][23].

CHAPTER 3

Theoretical Background

3.1 Equations

This section presents all underlying equations used in the design and optimisation process. In order to simplify the calculation process the propulsion system will be considered to be an ideal rocket. The ideal rocket case allows the relevant thermodynamic principles to be expressed as simple mathematical relationships. The valid assumptions of the ideal rocket case are listed in [1]. By using this case it is possible to use a quasi-one-dimensional model to describe the nozzle flow. However, while the assumptions and simplifications of the ideal rocket case are useful in preliminary design tasks, the complete system performance will usually exhibit an error between 1 and 6% below the calculated ideal value. All equations presented here have been sourced from [1] and [11], unless otherwise stated.

3.1.1 Engine Characteristics

The total thrust generated by the engine can be expressed as the following equation

$$F = C_F A_t p_c \tag{3.1}$$

Where F is the thrust of the engine, C_F is the thrust coefficient, A_t is throat area of the engine and p_c is the thrust chamber pressure.

The thrust coefficient C_F is calculated with

$$C_F = \sqrt{\frac{2\gamma_c^2}{\gamma_c - 1}\left(\frac{2}{\gamma_c + 1}\right)^{(\gamma_c+1)/(\gamma_c-1)}\left(1 - \left[\frac{p_e}{p_c}\right]^{(\gamma_c-1)/\gamma_c}\right)} + \frac{p_e - p_a}{p_c}\frac{A_e}{A_t} \quad (3.2)$$

where γ_c is the specific heat ratio of the combustion gases, p_e is the nozzle exit pressure, p_a is the ambient pressure outside the engine and A_e is the nozzle exit area.

The nozzle expansion ratio ε can be found with

$$\varepsilon^{-1} = \frac{A_t}{A_e} = \left(\frac{\gamma_c + 1}{2}\right)^{1/(\gamma_c+1)}\left(\frac{p_e}{p_c}\right)^{1/\gamma_c}\sqrt{\frac{\gamma_c + 1}{\gamma_c - 1}\left(1 - \left[\frac{p_e}{p_c}\right]^{(\gamma_c-1)/\gamma_c}\right)} \quad (3.3)$$

3.1.2 Propellant Flows

Mass flow $\dot{m}$ can be described by several useful expressions. Generally it is given by the mass conservation formula.

$$\dot{m} = \rho A U \quad (3.4)$$

Here A describes the exit area of the orifice and U is the bulk velocity of the fluid.

The total propellant mass flow $\dot{m}_{tot}$ can be expressed by

$$\dot{m}_{tot} = \frac{p_c A_t}{c^*} \quad (3.5)$$

where c^* is the characteristic velocity.

The relationships between the total propellant, the oxidiser and fuel mass flows are expressed by

$$\begin{cases} \dot{m}_{tot} = \dot{m}_o + \dot{m}_f \\ \\ OF = \dfrac{\dot{m}_o}{\dot{m}_f} \end{cases} \quad (3.6)$$

where the subscripts o and f represent oxidiser and fuel mass flows respectively. OF is the oxidiser to fuel ratio.

The density of gaseous propellant ρ_{gas} can be expressed by the ideal gas assumption

$$\rho_f = \frac{p_c}{R_f T_f} \quad (3.7)$$

R_{gas} is the gas constant of the propellant and T_{gas} is the injection temperature of the gas.

The velocity of an incompressible liquid is given by

$$U_{liq} = C_d \sqrt{\frac{2\Delta p}{\rho_{liq}}} \tag{3.8}$$

Where C_d is the discharge coefficient of the orifice, Δp is the pressure drop across the injector and ρ_{liq} is the density of the liquid propellant.

The velocity of a compressible gas can be calculated with

$$U_{gas} = C_d \sqrt{\frac{2R_{gas}T_{gas}\Delta p}{p_c}} \tag{3.9}$$

3.1.3 Injector Dimensions

The exit area of the pintle A_{pt} is calculated with

$$A_{pt} = L_{open}\pi(D_{pt} - 2\delta_{sleeve}) \tag{3.10}$$

where L_{open} is the opening distance of the pintle, D_{pt} is the diameter of the pintle tip and δ_{sleeve} represents the thickness of the pintle sleeve. The position of these dimensions can be seen in figure 2.4.

L_{open} is calculated via

$$L_{open} = \frac{L_{min}}{cos(\theta_{pt})} \tag{3.11}$$

Where θ_{pt} is the pintle tip angle, its position can be seen in figure 2.4, L_{min} represents the smallest distance between the surface of the pintle tip and the pintle sleeve. L_{min} can be found with the following equation

$$A_{min} = \pi(D_{pt} - 2\delta_{sleeve} - L_{min}sin(\theta_{pt}))L_{min} \tag{3.12}$$

where A_{min} is the minimum area between the pintle tip and the sleeve.

The area of the annular orifice is given by

$$A_{ann} = \pi\left(\left(\delta_{ann} + \left[\frac{D_{pt}}{2}\right]\right)^2 - \left[\frac{D_{pt}}{2}\right]^2\right) \tag{3.13}$$

where δ_{ann} is the annular gap thickness, its position can be found in figure 2.4.

3.1.4 Injector Performance

Sauter mean diameter D_{32} is calculated with

$$D_{32} = L_{open}\xi^{-1}\exp\left[4.0 - q\left(We^{0.1}\right)\right] \tag{3.14}$$

where

$$\begin{cases} \xi = \frac{90-\theta_{pt}}{90} \\ q = 3.455 - 0.225\xi \end{cases} \tag{3.15}$$

where We is the Weber number, which is calculated with

$$We = \frac{\rho_{gas} L_{open} (U_{gas} - U_{liq})^2}{\sigma_{liq}} \tag{3.16}$$

where σ_{liq} is the surface tension of the liquid.

Spray angle α is calculated with

$$\alpha = cos^{-1}\left(\frac{1}{1+TMR}\right) \tag{3.17}$$

Where TMR stands for the total momentum ratio, which is calculated with

$$TMR = \frac{\dot{m}_o U_o \cdot cos(\theta_{pt})}{\dot{m}_f U_f + \dot{m}_o U_o \cdot sin(\theta_{pt})} \tag{3.18}$$

Here it is assumed that the oxidiser is the central propellant and that the fuel is the outer propellant.

Vaporisation distance can be calculated with the following formula [5][11].

$$X = r_{d0}^2 \left[\frac{U_{d0}}{\sqrt{\gamma R_c T_c}} + \frac{3}{\Gamma}\frac{A_t}{A_c}\frac{\varphi}{10}\right] \frac{c_{p,c}\rho_o}{k_c} \frac{\sqrt{\gamma R_c T_c}}{\ln(1+B)} \frac{1}{(2+\varphi)} \tag{3.19}$$

in which

$$\Gamma = \left(\frac{\gamma+1}{2}\right)^{\frac{\gamma+1}{2(\gamma-1)}} \tag{3.20}$$

$$B = \frac{c_{p,c}(T_f - T_o)}{h_{fg}} \tag{3.21}$$

$$\varphi = \frac{9}{2}\frac{Pr_c}{B} \tag{3.22}$$

Where r_{d0} is the initial droplet radius, $c_{p,c}$ is the specific heat of the combustion gases, k_c is the thermal conductivity for the combustion gases, T_f is the injection temperature of the gaseous fuel, h_{fg} is the latent heat of vaporisation for the liquid and Pr_c is the Prandtl number of the combustion gases. This vaporisation formula produces the distance of vaporisation after the liquid sheet from the pintle injector has been broken up, if one wishes to acquire the vaporisation distance from the pintle tip the breakup of the liquid sheet would also have to be modelled. A_c is the cross sectional area of the combustion chamber and can be found by assuming a reasonable value for the contraction ratio (A_C/A_t), a value of 13 is reasonable for a pintle injector engine [24].

3.1.5 Optimisation

The general cost function is expressed by the following formula [25].

$$J = \begin{bmatrix} x_1 \\ x_2 \\ \vdots \\ x_n \end{bmatrix}^T \begin{bmatrix} Q_1 & 0 & \cdots & 0 \\ 0 & Q_2 & \cdots & 0 \\ \vdots & \vdots & \ddots & \vdots \\ 0 & 0 & \cdots & Q_n \end{bmatrix} \begin{bmatrix} x_1 \\ x_2 \\ \vdots \\ x_n \end{bmatrix} \tag{3.23}$$

where J is the cost of the system, x is a vector containing the states of the system and Q is a weighting matrix.

The minimum value is of interest, and can be found with

$$\min_x(J) \rightarrow \frac{\partial J}{\partial x} = 0 \tag{3.24}$$

CHAPTER 4

Initial Conditions

4.1 Performance Parameters

Performance parameters is the name given to the parameters that the design will aim to optimise, selecting these parameters will be highly dependant of the specific project requirements. In this project the following parameters are deemed to be of interest: minimising droplet sizes expressed through SMD, maximising the spray angle of the injected propellants and minimising vaporisation distance of the droplets. These were chosen since they should be very important parameters to the vast majority of engine designs.

4.2 Thrust

The first step in designing rocket engine components is to decide the thrust capability of the engine, usually this is decided by the demands of the mission [6]. For this thesis the thrust was limited by the scale of the project and was chosen based on what other small scale projects have been able to achieve. In the end a max thrust of 1000N was selected. It is also decided that the injector should be capable of deep throttling, this means it must be capable of a minimum thrust of 200N. The injector shall also contain five discrete throttle levels as design points, these are placed at 200N, 400N, 600N, 800N and 1000N.

4.3 Chamber Pressure

The next step was to decide the thrust chamber pressure (p_c). Chamber pressure has a strong impact on the performance of the rocket, where higher pressure usually mean better combustion performance. However, higher chamber pressure also mean more structural strain on the thrust chamber which has to be offset by a stronger thrust chamber which adds more weight. It also means more complexity in general because the propellant feed system also has to be able to withstand the higher pressure. This means that a trade-off has to be made here which is usually based on the thrust of the engine, where smaller engines have lower pressures and higher thrust engines have higher chamber pressures [6]. Because of the relatively low max thrust selected previously a max chamber pressure of 20 bar was chosen.

4.4 Movable Pintle and Movable Sleeve

A moving pintle type design was chosen for this project. While the advantage of a moving sleeve design is great, as described in section 2.3.2, the added complexity in its design is deemed to be unnecessary for this project.

4.5 Propellants

In section 2.6 various propellants were described. From these LOX and methane were selected as propellants for this design. This combination was selected due to a few key points:

- It is a relatively safe combination of propellants and its combustion products are non-toxic.
- Methane has a lot of research potential and there is currently great interest in designing methane fuelled rockets.
- LOX has well proven heritage and is therefore a safe choice for oxidiser.

Since a movable pintle design was selected it is beneficial to use a gas/liquid combination. A gaseous propellant won't require area control in order to maintain optimal injector pressure and should therefore be the outer annular propellant [11]. Methane is selected as the gaseous propellant since the combustion process will require more oxidiser by mass, it is therefore beneficial for it to be in liquid form. This means that the pintle will be an oxidiser centred one.

4.5.1 Oxidiser to Fuel Ratio

In order to find the optimal oxidiser to fuel (OF) ratio of the propellants one must first analyse the combustion reaction of the chosen propellant combination.

Methane and oxygen react according to the following formula during combustion.

$$CH_4 + 2O_2 \rightarrow CO_2 + 2H_2O \tag{4.1}$$

Next the ratio between the molecular weights of the combustion reactants is calculated.

$$\frac{O}{F} = \frac{2 \cdot 2 \cdot 16}{12 + 4 \cdot 1} = 4 \tag{4.2}$$

This is called the stoichiometric ratio and is the ratio where complete combustion takes place, at this ratio all reactants are fully consumed. The release of energy per unit mass of propellant mixture and the combustion temperature are highest at or near the stoichiometric mixture. In practice however this is most often not the best OF ratio, a more fuel rich mixture generally has a lower molecular weight which increases specific impulse [1]. A fuel rich mixture also has the added benefit of reducing the risk of unburnt oxidiser which will minimise damage to the engine [6].

For this project the optimal OF ratio is decided to be the one that provides the highest characteristic velocity (c^*).

In order to find the optimal OF ratio a lot of complex chemical calculations have to be performed, in order to perform these the NASA program CEA (Chemical Equilibrium and Applications) will be utilised. CEA is a program which calculates chemical equilibrium product concentrations from any set of reactants and determines thermodynamic and transport properties for the product mixture. it is a very powerful program with built in applications to calculate theoretical rocket performance [26][27]. CEA will be utilised in multiple parts of the design process.

The first step is to set a thrust level to have optimal expansion, this is when the exit pressure of the nozzle equals ambient pressure which provides maximum performance, here the maximum thrust level is set to be optimally expanded. With this assumption CEA can calculate c^* for a range of OF ratios and the following graph is created.

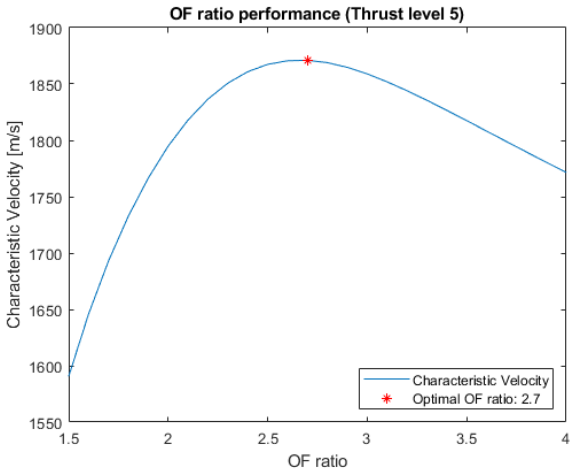

Figure 4.1: Characteristic velocity vs oxidiser to fuel ratio for maximum thrust level. This shows how c^* changes with OF ratio, the red asterisk marks the optimal OF ratio of 2.7.

From this plot a optimal OF ratio of 2.7 is acquired, giving a c^* of 1871.0 m/s. The optimal fuel ratio changes with different thrust chamber pressures and will thus have to be recalculated for other thrust levels.

4.6 Mass Flows

The goal of this section is to acquire the propellant mass flows that are required for all thrust levels.

1. First the specific heat ratio and the characteristic velocity of the maximum thrust level is acquired through CEA. This case is defined by the max thrust set in section 4.2, the max chamber pressure from section 4.3, the optimal OF ratio from figure 4.1 and the assumption of optimal expansion.

2. After this the thrust coefficient C_F can be calculated with equation 3.2. Since optimal expansion is assumed p_e is considered equal to p_a, which is set to be equal to atmospheric pressure.

3. Next, equation 3.1 is solved for the nozzle throat area A_t.

4. Now equation 3.5 can be solved for the maximum thrust level. This equation will give the total mass flow required to achieve the desired maximum thrust.

The steps taken in 1-4 only work if optimal expansion can be assumed. However, since the nozzle geometry can't change for each thrust level it is only possible

to achieve optimal expansion for one thrust level unless the ambient pressure changes. This means a couple of extra steps have to be added in order to find the propellant mass flows for all thrust levels.

5. By using equation 3.3 the nozzle expansion ratio (ε) can be calculated. The values used here are those of the optimally expanded maximum thrust level.

6. With the nozzle expansion ratio CEA can be used without assuming optimal expansion.

7. In order to find the values for the lower thrust levels it is assumed that thrust and chamber pressure is directly proportional, meaning dropping p_c to 80% will also drop F to 80%.

This is an incorrect assumption but it is a good starting point, one can see from equation 3.1 that thrust is dependant on C_F, A_t and p_c. A_t is a fixed chamber geometry parameter and will thus be unchanged regardless of p_c, C_F will change based on the properties of the exhaust gasses which will be slightly influenced by a change in p_c. However this change will be small compared to the change in p_c. Additional tuning of this assumption will be required once the resulting thrust has been calculated, for now the following values for p_c are used in CEA.

Thrust level	Chamber Pressure [bar]	Desired Thrust [N]
1	4 (20% of max p_c)	200
2	8 (40% of max p_c)	400
3	12 (60% of max p_c)	600
4	16 (80% of max p_c)	800
5	20 (max p_c)	1000

Table 4.1: Initial assumptions for chamber pressures and the desired thrust, column two shows the assumed pressure values described in step 7.

8. Next the optimal OF ratios of thrust levels 1-4 are found by calculating the characteristic velocity for different OF ratios in CEA. The nozzle expansion ratio from step 5 and the assumptions made in step 7 are applied here. The results can be seen in figure 4.2.

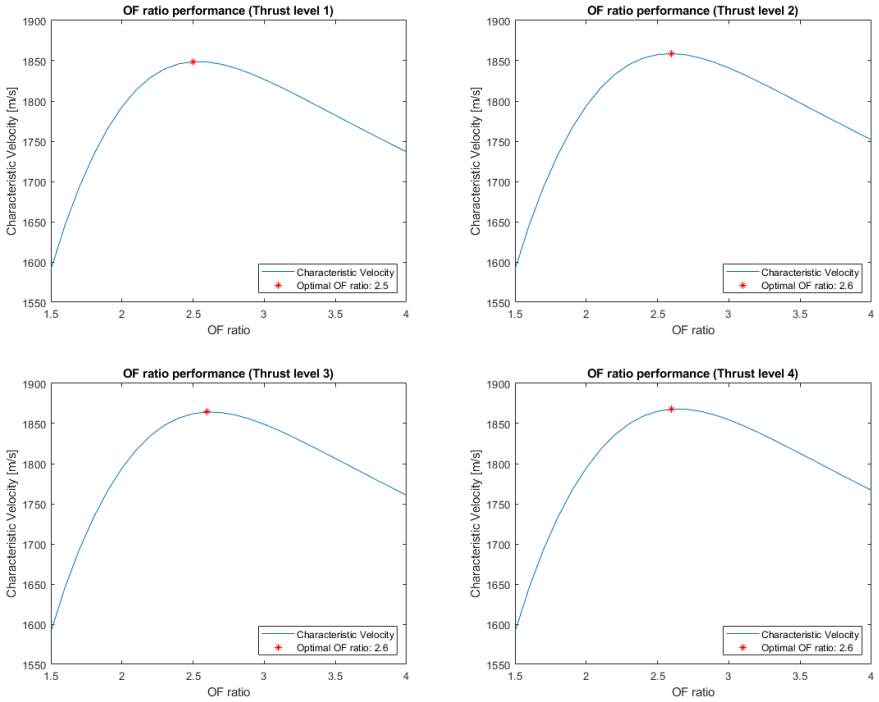

Figure 4.2: Characteristic velocity vs oxidiser to fuel ratio for thrust levels one through four. The red asterisk marks the optimal OF ratio for each thrust level.

9. Now CEA can calculate the specific heat ratio (γ_c) for thrust levels 1-4. The nozzle expansion ratio from step 5, the chamber pressure assumptions from step 7 and the OF ratios from figure 4.2 are used in this calculation.

10. Next the exit pressure of thrust levels 1-4 can be calculated by solving equation 3.3 numerically with respect to p_e.

11. By using equation 3.2 with ε from step 5, γ_c from step 9 and p_e from step 10 the thrust coefficient of thrust levels 1-4 can be calculated.

12. Now equation 3.1 can be used to calculate the actual thrust for each thrust level, the results can be seen in table 4.2. This step checks the quality of the assumption made in step 7.

Thrust level	Chamber Pressure [bar]	Desired Thrust [N]	Calculated Thrust [N]
1	4 (20% of max p_c)	200	90.71
2	8 (40% of max p_c)	400	318.3
3	12 (60% of max p_c)	600	545.6
4	16 (80% of max p_c)	800	772.9
5	20 (max p_c)	1000	1000

Table 4.2: Calculated thrust levels for the initial p_c assumption. Note the difference between the desired and calculated thrust, this difference indicates that the assumption made in step 7 is poor.

The poor correlation between the desired and calculated thrust in table 4.2 is due to the quality of the p_c assumption made in step 7. This was expected and the assumption must be tuned in order to achieve acceptable thrust. This tuning will consist of repeating steps 7-12 while changing the p_c values in step 7 for each repetition. If the calculated thrust in step 12 is too low the value of p_c should be increased and if the thrust is too high the p_c value should be lowered. Steps 7-12 will be repeated until the desired and calculated thrust are within acceptable margins for all thrust levels.

After this tuning process the graphs obtained in step 8 are amended with the new values of characteristic velocity that arise from the changed chamber pressure. The amended graphs can be seen in figure 4.3. The optimal OF ratios that are obtained in these graphs are considered to be the final OF ratios and won't be changed after this.

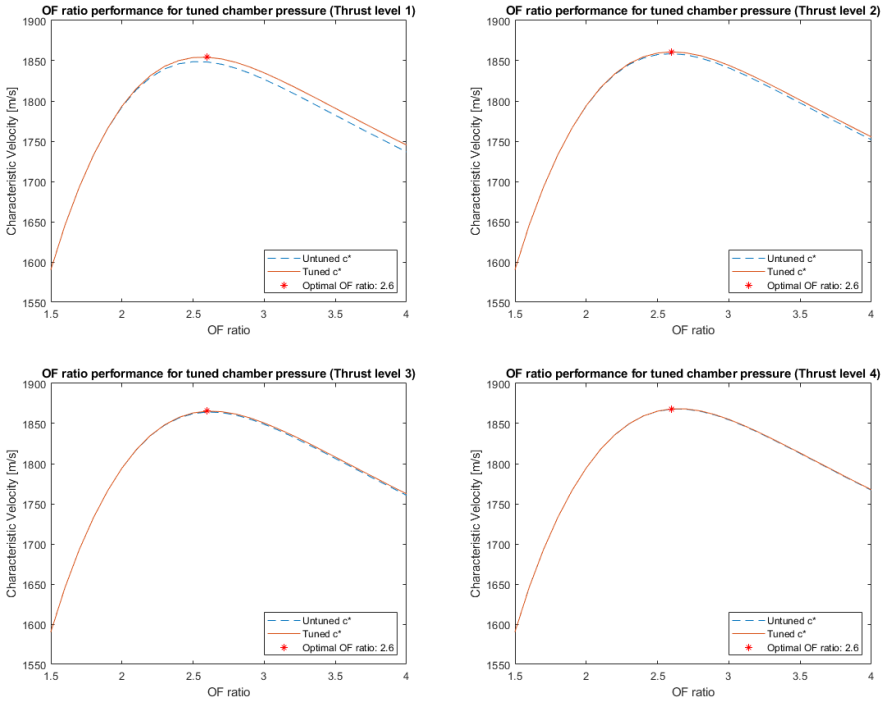

Figure 4.3: Characteristic velocity vs oxidiser to fuel ratio for thrust levels one through four after tuning. The red asterisk marks the optimal OF ratio for each thrust level.

The calculated thrust levels of step 12 after tuning are presented in table 4.3.

Thrust level	Chamber Pressure [bar]	Desired Thrust [N]	Calculated Thrust [N]
1	5.9 (29.5% of max p_c)	200	200.9
2	9.4 (47% of max p_c)	400	398.9
3	13 (65% of max p_c)	600	602.6
4	16.4 (82% of max p_c)	800	794.8
5	20 (max p_c)	1000	1000

Table 4.3: Final p_c values. The desired and calculated thrust values show good correlation here, indicating that the p_c values are at a good level.

Table 4.3 presents the tuned values for p_c and the thrust levels they produce, there is still a slight error between the desired and calculated values. However this error is below 1% for all thrust levels, which is deemed to be acceptable. Figure 4.3 shows the new optimal OF ratios after tuning. By taking the values for c^* calculated by CEA for the final p_c values one can calculate the total propellant mass flow ($\dot{m}_{tot}$) for all thrust levels.

13. Next the total propellant mass flow rate ($\dot{m}_{tot}$) can be calculated using equation 3.5 with A_t from step 3, tuned p_c values from table 4.3 and the tuned c^* from step 8.

14. Finally the oxidiser and fuel flow rates can be acquired by solving the system of equations in 3.6 with respect to $\dot{m}_o$ and $\dot{m}_f$. The OF ratios from figure 4.3 and the $\dot{m}_{tot}$ values from the previous step are applied here. The final mass flow values can be seen in table 4.4.

Thrust level	Oxidiser mass flow [kg/s]	Fuel mass flow [kg/s]
1	0.0811	0.0312
2	0.1288	0.0495
3	0.1777	0.0683
4	0.2238	0.0861
5	0.2754	0.1020

Table 4.4: Oxidiser and fuel mass flow for all thrust levels. The mass flows presented here show the mass flows that are required to achieve the desired thrust.

The oxidiser and fuel mass flows presented in table 4.4 show the mass flows that the injector must be able to support. The values of these mass flows will therefore be used as requirements on the injector as it is being designed in the next chapter.

CHAPTER 5

Design Process

This section describes the process of designing and optimising the outlet region of the pintle injector.

5.1 Finding Fundamental Variables

First the design variables that influence the performance parameters must be found. This is done by starting with the equation that describes the performance and then working backwards to find the fundamental relationships that impact that specific performance parameter. From these the ones that can be changed by the design are identified and will be considered to be design variables. If a performance parameter is found to be dependant on a variable that has been set as a requirement (for instance $\dot{m}_o$) the impact of this variable will not be considered, since changing this would impact the requirements.

5.1.1 SMD Design Variables

SMD is given by equation 3.14. Working backwards from this equation it can be found that the relevant variables that can be changed by the design are pintle tip diameter (D_{pt}), pintle tip angle (θ), annular gap thickness δp_{ann}, pressure drop across the pintle Δ_{pt} and the pressure drop across the annular orifice Δp_{ann}

5.1.2 Spray Angle Design Variable

Spray angle is described in equation 3.17, which is dependant on TMR from equation 3.18. The design variables identified here are θ, δ_{ann}, Δp_{pt} and Δp_{ann}.

5.1.3 Vaporisation Distance Design variables

The vaporisation distance is calculated with equation 3.19. By analysing this equation one can see that the majority of the variables here are dependant on the chemical composition of the propellants and combustion gases. These variables are governed by processes that are considered to be requirements. The variables that can be influenced by the injector design are the initial droplet size and velocity. It is assumed that the droplet will quickly be accelerated by the impinging gas and that the initial droplet velocity (U_{d0}) therefore can be considered equal to the fuel injection velocity [28]. The initial droplet size is assumed to be equal to the SMD [11]. Because of this assumption it will share its design variables with SMD giving vaporisation distance the following design variables: D_{pt}, θ, δ_{ann}, Δp_{pt} and Δp_{ann}

5.1.4 Design Variable Summary

In summary, the design variables will include the following five variables: D_{pt}, θ, δ_{ann}, Δp_{pt} and Δp_{ann}. It is not immediately apparent exactly how all of these design variables will impact the final performance values. It is therefore necessary to find a way to evaluate these variables.

5.2 Impact Evaluation

By constructing a theoretical injector with semi arbitrary initial dimensions and then varying each of the five design variables one by one their influence on the key performance parameters (spray angle, SMD and vaporisation distance) can be evaluated. It is desirable to maximise spray angle and minimise SMD and vaporisation distance. This injector is modelled in a MATLAB program.

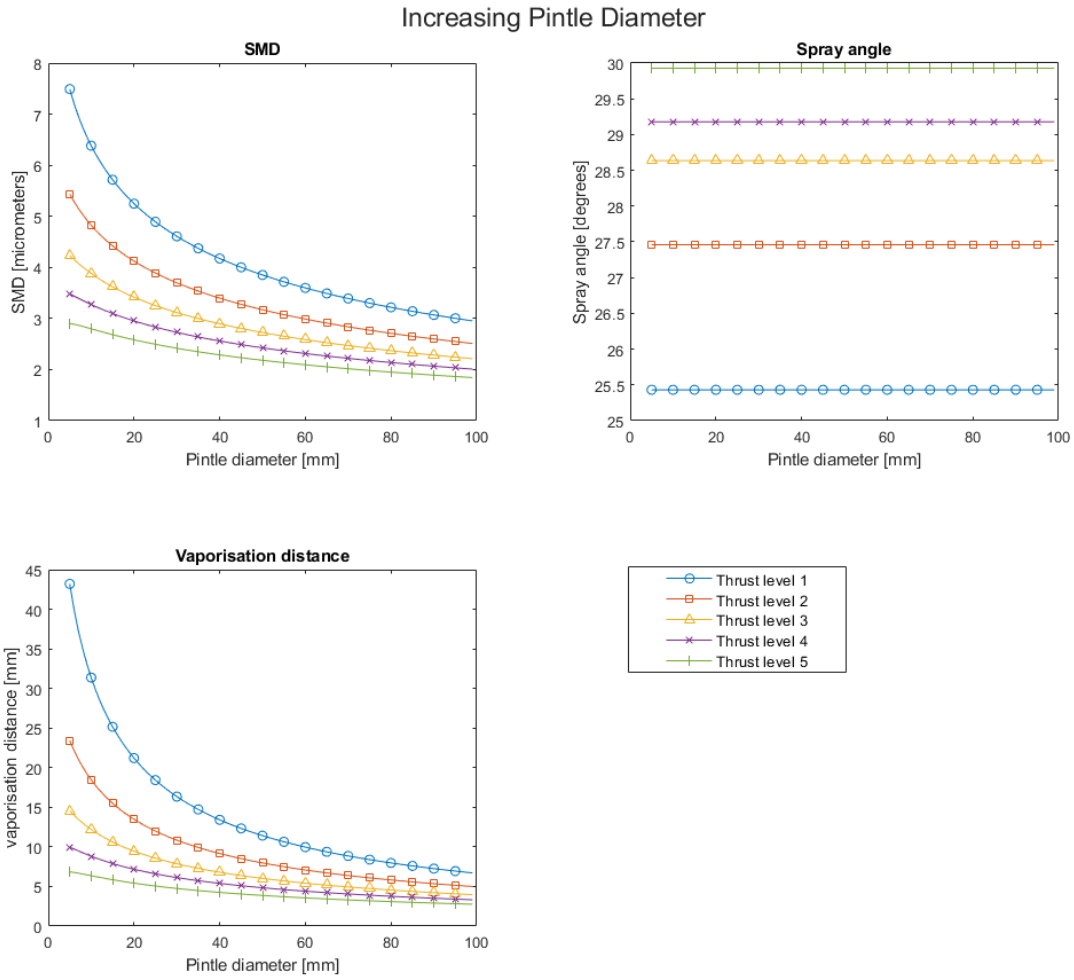

Figure 5.1: Increasing pintle tip diameter D_{pt} will decrease both SMD and X while leaving α unchanged. indicating larger pintle tip diameters are preferred.

Figure 5.1 shows that increasing the pintle tip diameter will decrease both SMD and vaporisation distance. This is desirable and shows that larger pintle tip diameters are preferred. Figure 5.1 also shows that the pintle tip diameter will have no impact on the spray angle.

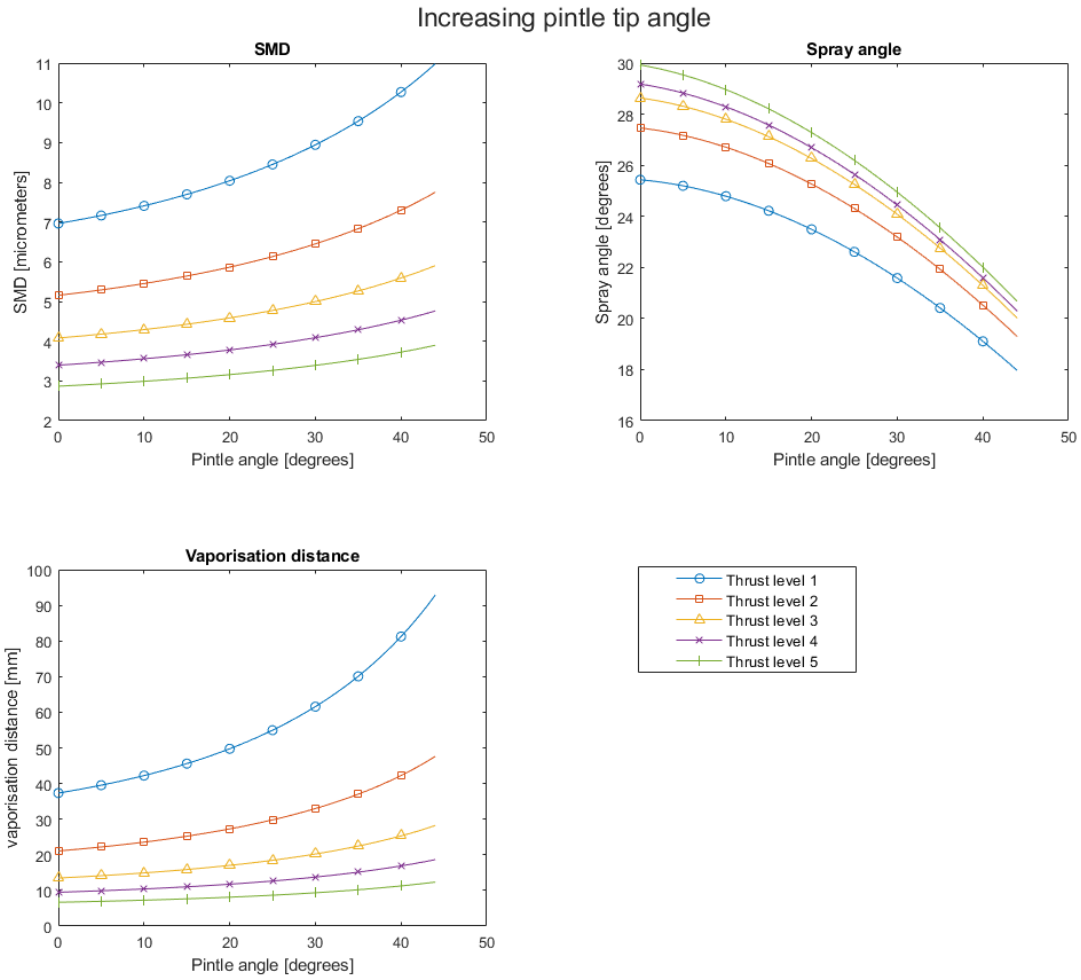

Figure 5.2: Increasing pintle tip angle θ_{pt} will increase both SMD and X while decreasing α. Indicating that lower pintle tip angles are preferred.

In figure 5.2 one can see that as the pintle tip angle is increased both SMD and vaporisation distance is also increased. This is undesirable since smaller droplet sizes and shorter vaporisation distances are preferred. The spray angle is also affected in a negative way. As the pintle tip angle is increased the spray angle will decrease, this is undesirable since larger spray angles are preferred. The graphs in figure 5.2 show that when looking at these three performance parameters lower pintle tip angles are preferred.

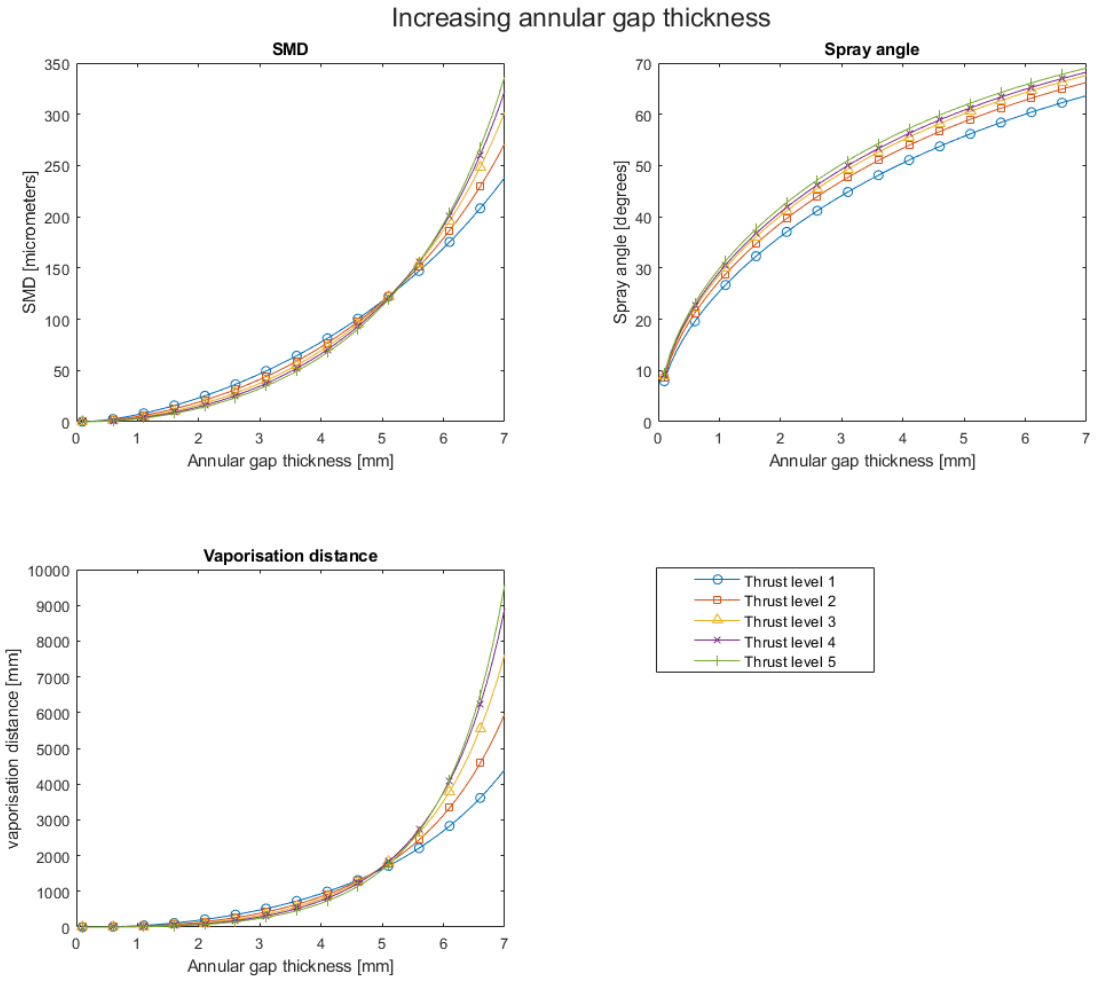

Figure 5.3: Increasing the annular gap thickness δ_{ann} will increase SMD, α and X. This is beneficial to α but not to SMD and X.

In figure 5.3 one can see that all performance parameters are increased as the annular gap is increased. This is beneficial to the spray angle but not to SMD and vaporisation distance. This indicates that a compromise has to made when deciding the optimal value for the annular gap since its effects are both negative and positive.

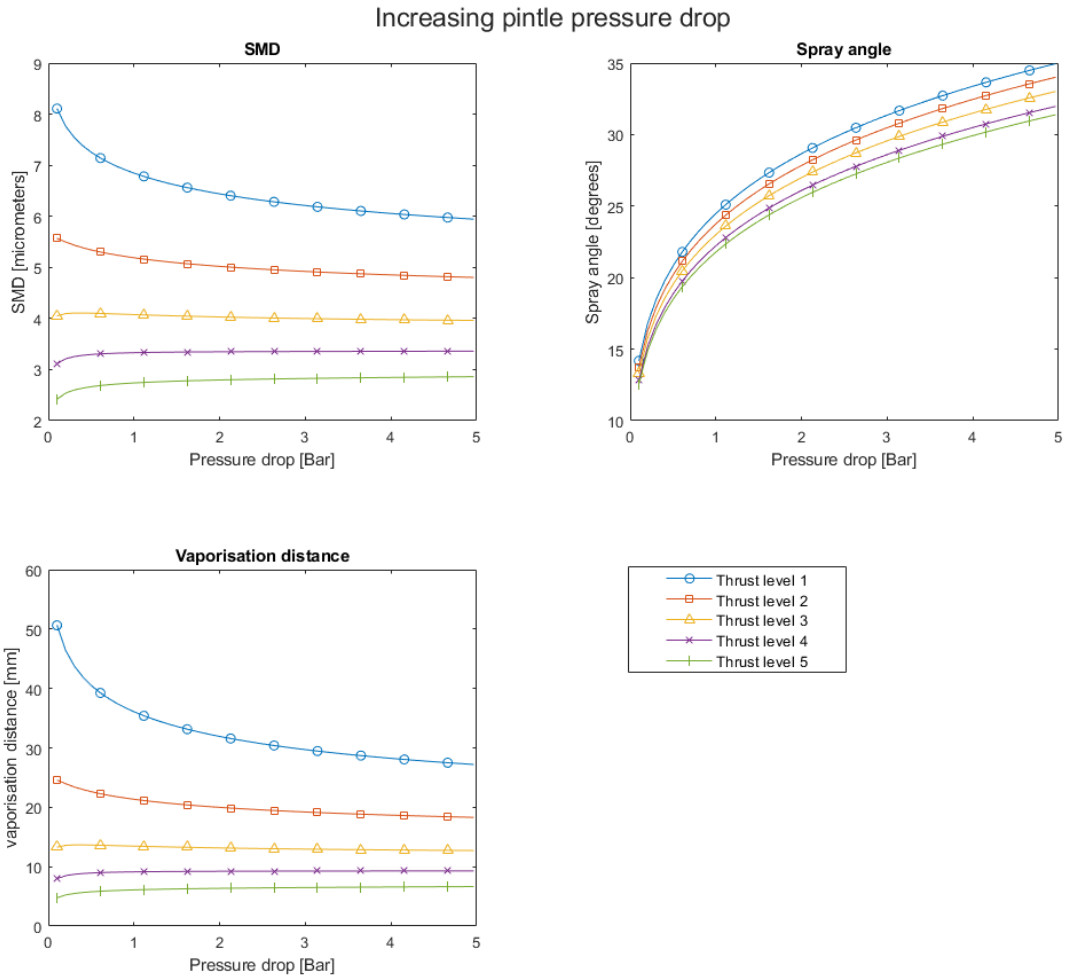

Figure 5.4: Increasing pintle pressure drop will decrease SMD and X for lower thrust levels while slightly increasing them for higher thrust levels. α will increase for all thrust levels.

The graphs in figure 5.4 show an interesting trend for SMD and vaporisation distance. As the pressure drop increases SMD and vaporisation distance will decrease for lower thrust levels but will very slightly increase for higher thrust levels. It can also be seen that the spray angle will increase as the pressure drop increases. This shows that a compromise is necessary when deciding the value of the pintle pressure drop.

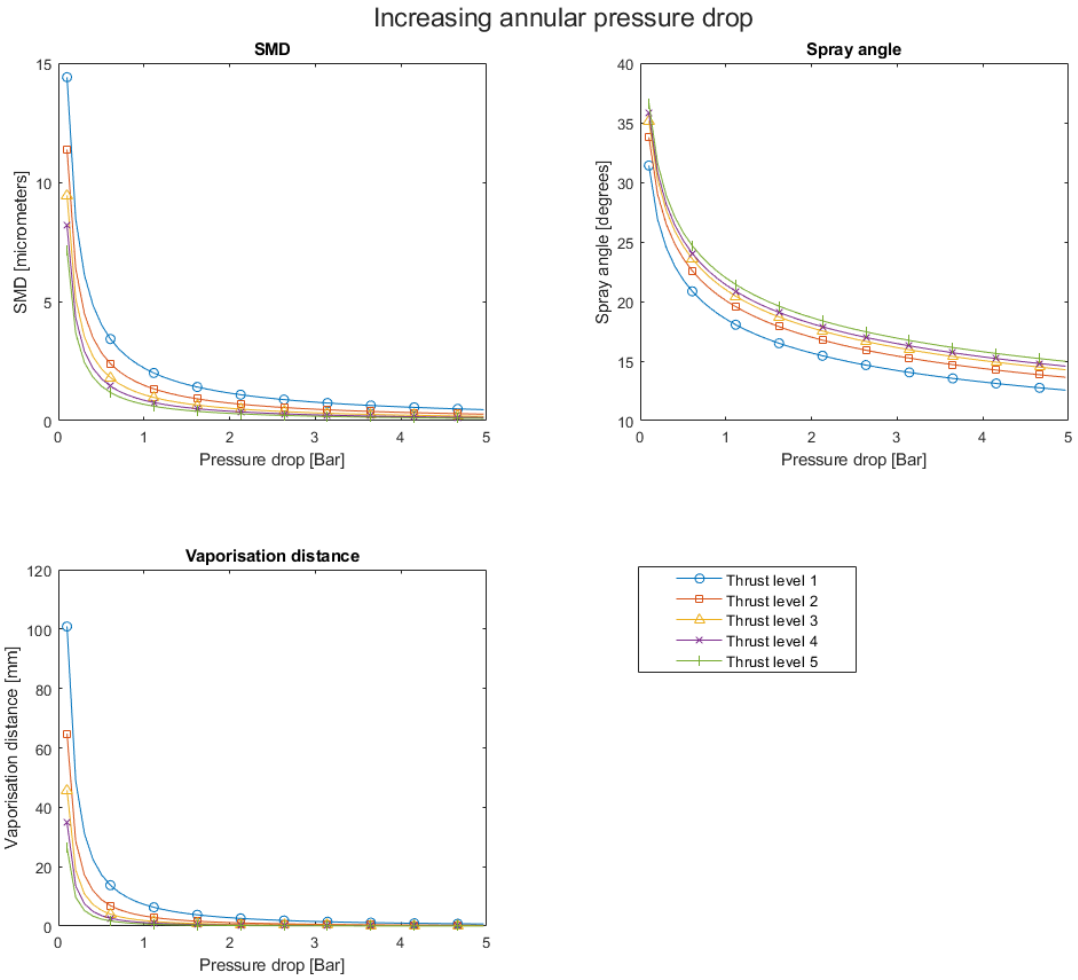

Figure 5.5: Increasing the annular pressure drop will decrease SMD, α and X. This is beneficial to SMD and X but not to α.

Figure 5.5 shows that the value of all performance parameters are decreased as the annular pressure drop is increased. This is beneficial to both SMD and the vaporisation distance but not to the spray angle. This means a compromise has to be made when deciding the value of the annular pressure drop.

5.2.1 Summary of Evaluation

A summary of the graphs in section 5.2 can be seen in table 5.1.

	D_{pt}	θ_{pt}	δ_{ann}	Δp_{pt}	Δp_{ann}
SMD	+	-	-	+/-	+
X	+	-	-	+/-	+
α		-	+	+	-

Table 5.1: Summary of the design variable effects on the performance parameters. The plus and minus signs indicate if that columns design variable will have a negative or positive impact on the corresponding performance parameter.

The plus and minus signs in table 5.1 indicate if the design variable has a positive or negative impact on each performance parameter. If a column only contains negative signs it indicates that increasing this particular design variable has a strictly negative impact on the injector performance and should be minimised. If a column contains both negative and positive signs it indicates that the design variables are in conflict with each other. Since several of the design variable columns in table 5.1 contain both plus and minus signs it indicates that several design variables are in conflict. This means it is not possible to construct a single injector outflow region in a way that provides the optimal performance for the entire set of performance parameters, a compromise has to made when designing the injector. In order to find the best compromise it is useful to translate the various parameters into an optimisation problem.

5.3 Optimisation problem

5.3.1 The Cost Function

In order to find the best compromise a cost function is constructed. A cost function is a way to assign a scalar value to a complex system of several states in order to be able to easily compare several options. The cost function is frequently used in the field of optimal control theory, where it can be used to find the best compromise between controller performance and actuator effort [25]. The basic cost function is shown in equation 3.23. In equation 3.23 x represents the states of the system being evaluated, in this design process these will be replaced by the performance parameters being optimised. Q is a weighting matrix, by changing the values here one can influence the impact x_1, x_2 ... x_n have on the final value of J. Q can be seen as a set of tuning knobs that can be used to influence the trade-off between the different performance parameters. J is a scalar value and is considered to be the "cost" of a particular design variable configuration. The optimal configuration is then the one with the lowest associated cost, the smallest J value [25].

A few changes to the general cost function 3.23 are made in order to adapt it to this design process. It is desirable to maximise the spray angle (α) but since the general cost function is designed to find the minimum value this parameter must be modified. By changing the sign of the part of the cost function related

to the spray angle larger spray angles values will have a minimising effect on the overall cost function value.

$$\max_{\alpha}(J) \rightarrow \min_{\alpha}(-J) \tag{5.1}$$

This change can be accomplished by changing the spray angle weighting cost to be negative.
In addition to this, the Q_{level} is also added, this will enable weighting of individual thrust levels. This is added since one often want better performance at higher thrust levels since greater efficiency at higher mass flow will yield greater amounts of saved propellants. This number is set to be equal to its corresponding thrust level ($Q_{level} = 5$ for thrust level 5, $Q_{level} = 4$ for thrust level 4, ...), basically weighting the function in favour of the performance at higher thrust levels. With these changes the following cost function is constructed.

$$J = Q_{level} \begin{bmatrix} D_{32} \\ \alpha \\ X \end{bmatrix}^T \begin{bmatrix} Q_D & 0 & 0 \\ 0 & -Q_\alpha & 0 \\ 0 & 0 & Q_X \end{bmatrix} \begin{bmatrix} D_{32} \\ \alpha \\ X \end{bmatrix} \tag{5.2}$$

The cost function can now be applied to the design process.

5.3.2 Application of Cost Function

In order to find the optimal design every possible combination of the key design variables D_{pt}, δ_{ann}, θ_{pt}, Δp_{pt} and Δp_{ann} has to be considered. By using the formulas in sections 3.1.3 and 3.1.4 an optimisation algorithm is constructed in MATLAB that applies the cost function 5.2 to every combination of the design variables being investigated. Here the parameters are also constrained to reasonable values. By comparing the costs of each combination, the best injector configuration can be found by selecting the one with the lowest associated cost.

The constraints of the design program are as follows:

- D_{pt} is limited to be no smaller than $5mm$ and no larger than $100mm$. Smaller pintle tips are deemed to be unfeasible and larger tips to be excessively large.
- δ_{ann} is limited to be no smaller than $0.01mm$ and no larger than $6mm$. Smaller annular gap thicknesses are deemed to be unfeasible and larger gaps to be excessively large.
- L_{open} must be larger than $0.1mm$. Previous research found that opening distances lower than this had trouble in forming a uniform liquid sheet out of the pintle tip [29].
- $\Delta p/p_c$ must be between 0.05 and 0.3. This ratio is as a general rule of thumb usually set at around 20%, higher values mean more costly pressure machinery and lower values induce a risk of detrimental effects, such as

chug, in the injector and feed systems. Engines with this ratio as low as 5% have been demonstrated and is therefore set as the lowest limit [6].

- Propellant injection velocities must be below the local sonic velocity. Supersonic flow can be quite dangerous within the thrust chamber and is undesirable.

With these constraints the MATLAB algorithm can be used to rapidly construct different injector configurations by simply choosing the values of Q in equation 5.2. The Q values selected here will impact how much weight is put on each performance parameter and it is up to the algorithm user to select appropriate Q values and evaluate which weighting produces the best injector. The following flowchart describes the overall function of the optimisation algorithm.

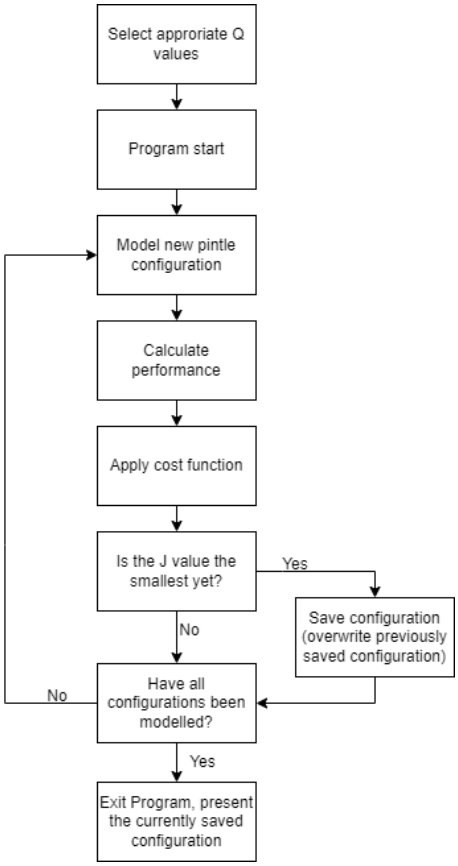

Figure 5.6: Flowchart of optimisation algorithm function

5.4 Q Value Impact

In order to investigate how different Q values impact the results of the optimisation algorithm a series of surface plots are constructed. The vertical axis in these represent the value of the performance parameter of the optimised injector configuration from the algorithm. The horizontal axes represent the size of the Q values. In each plot a pair of Q values are investigated, the third Q is kept at a constant value of 1. Once plots of all possible pairings have been made insight will be gained into how the size of each Q value impacts the performance parameters of the optimised injector configuration.

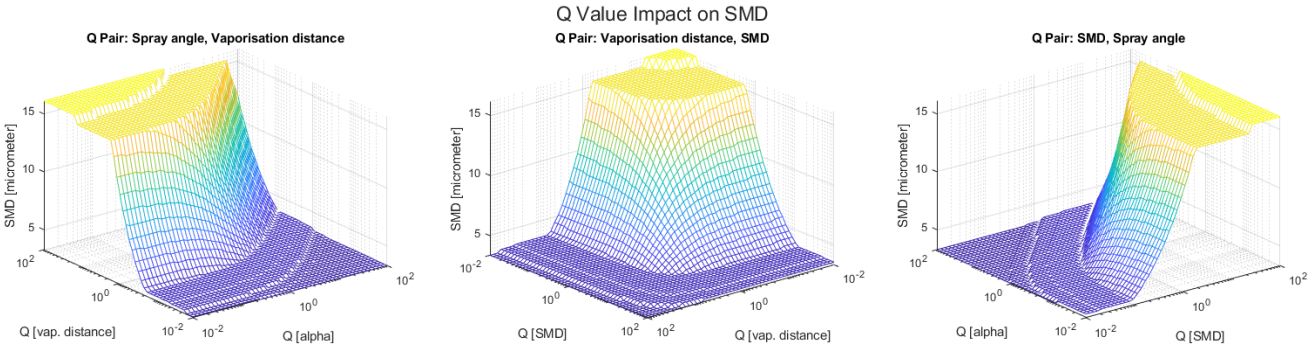

Figure 5.7: Impact of different Q values on optimisation algorithm SMD performance. The slope shows the area where changing Q values will have an impact on the final result.

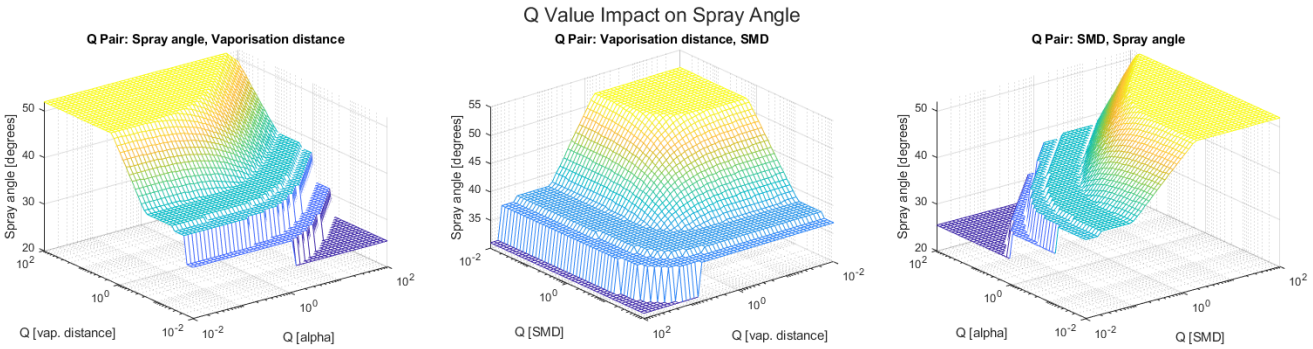

Figure 5.8: Impact of different Q values on optimisation algorithm spray angle performance. The slope shows the area where changing Q values will have an impact on the final result.

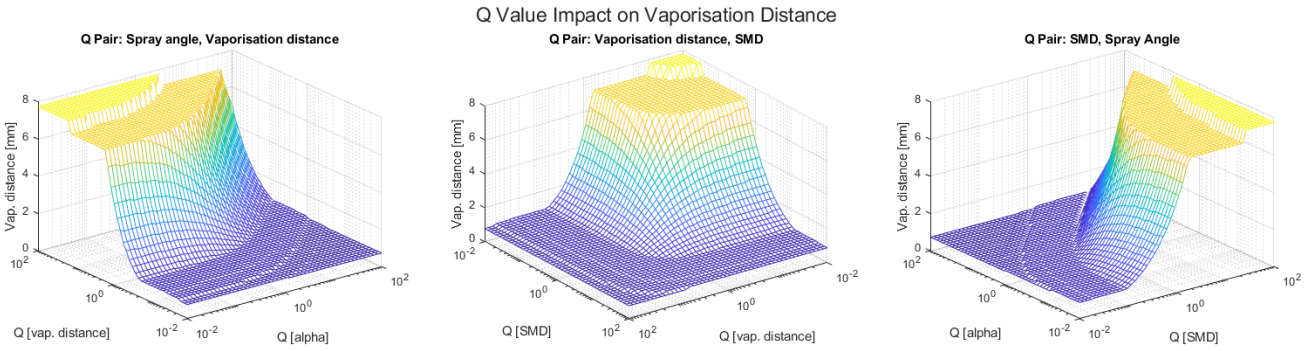

Figure 5.9: Impact of different Q values on optimisation algorithm vaporisation distance performance. The slope shows the area where changing Q values will have an impact on the final result.

In general these surface plots show a sloped region and flat areas on the edges of the slope. The flat areas arise when the optimisation algorithm runs into one of the constraints set in section 5.3.2, the Q values are saturated here. One should place the Q values on the slope of the surface plots as this is the area where different values will have the greatest impact on the resulting performance parameters. By analysing these plots one can see that Q values placed between roughly 0.1 and 10 will place the algorithm results on the slope. This range can therefore be considered appropriate and Q values should be within this range in order for the algorithm to function properly. However, extra care should be taken when using values at the ends of this range as they may still saturate the algorithm depending on the other selected Q values. With this knowledge the algorithm can be used to generate designs.

Here the result of a few different Q values are shown in order to demonstrate the versatility of the optimisation algorithm.

Injector 1: SMD optimised ($Q_D = 1$, $Q_\alpha = 0$, $Q_X = 0$)
By using these Q values the resulting injector will be optimised for SMD. Since their corresponding Q values are set to zero spray angle and vaporisation distance will have no impact on the final value of J in equation 5.2. This means that this injector should have the smallest possible SMD of all possible configurations constructed by the algorithm.

Thrust level	D_{pt} [mm]	θ_{pt} [degrees]	δ_{ann} [mm]	Δp_{pt} [bar]	Δp_{ann} [bar]
1	44	0	0.24	0.295	1.76
2	-	-	-	0.470	2.78
3	-	-	-	0.650	3.83
4	-	-	-	0.820	4.82
5	-	-	-	1.000	5.55

Table 5.2: Configuration for injector where only SMD optimisation is considered.

Which results in the following performance.

Thrust level	SMD [μm]	α [degrees]	X [mm]
1	6.359	18.48	2.695
2	4.969	20.68	1.689
3	4.109	22.34	1.178
4	3.552	23.61	0.8928
5	3.271	25.49	0.7267

Table 5.3: Performance of SMD optimised injector configuration. The SMD values of this table will be the smallest of all configurations.

Injector 2: spray angle optimised ($Q_D = 0$, $Q_\alpha = 1$, $Q_X = 0$)
By using these Q values the resulting injector will be optimised for spray angle. Since their corresponding Q values are set to zero SMD and vaporisation distance will have no impact on the final value of J in equation 5.2. This means that this injector should have the largest possible spray angle of all possible configurations constructed by the algorithm.

Thrust level	D_{pt} [mm]	θ_{pt} [degrees]	δ_{ann} [mm]	Δp_{pt} [bar]	Δp_{ann} [bar]
1	12	0	1.81	1.77	0.317
2	-	-	-	2.82	0.502
3	-	-	-	3.90	0.691
4	-	-	-	4.92	0.869
5	-	-	-	6.00	1.00

Table 5.4: Configuration for injector where only spray angle optimisation is considered.

Which results in the following performance.

Thrust level	SMD [μm]	α [degrees]	X [mm]
1	25.56	40.42	18.96
2	22.16	44.29	14.68
3	19.97	47.07	12.17
4	18.51	49.08	10.63
5	18.28	51.93	9.957

Table 5.5: Performance of spray angle optimised injector configuration. The spray angle values of this table will be the largest of all configurations.

Injector 3: SMD favoured ($Q_D = 5$, $Q_\alpha = 1$, $Q_X = 0$)
In this injector configuration SMD values are heavily favoured as the SMD Q value is higher compared to the other performance parameters.

Thrust level	D_{pt} [mm]	θ_{pt} [degrees]	δ_{ann} [mm]	Δp_{pt} [bar]	Δp_{ann} [bar]
1	19	0	0.57	1.77	1.59
2	-	-	-	2.82	2.52
3	-	-	-	3.90	3.47
4	-	-	-	4.92	4.36
5	-	-	-	6.00	5.02

Table 5.6: Configuration for SMD favoured injector. This injector would be used when compromise between SMD and spray angle is necessary and SMD is considered more critical.

Which results in the following performance.

Thrust level	SMD [μm]	α [degrees]	X [mm]
1	7.059	28.69	3.164
2	5.643	31.85	2.076
3	4.759	34.19	1.505
4	4.182	35.93	1.179
5	3.922	38.48	0.996

Table 5.7: Performance of SMD favoured injector configuration. Due to the weighting SMD values here are close to those in table 5.3, but slightly worse

This Injector configuration showcases a design where SMD values are highly favoured but is not the only performance parameter being considered. Due to the high SMD weighting factor SMD of table 5.7 will be very close to those of table 5.3. But due to the fact that spray angle is also being considered the SMD values will be slightly worse than the injector where only SMD is being considered. However due to the spray angle weighting in injector 3 its spray angles will be larger than that of the SMD optimised configuration.

Injector 4: Spray angle favoured ($Q_D = 1$, $Q_\alpha = 3$, $Q_X = 1$)
In this injector configuration spray angle is favoured as the spray angle Q value is higher compared to the other performance parameters.

Thrust level	D_{pt} [mm]	θ_{pt} [degrees]	δ_{ann} [mm]	Δp_{pt} [bar]	Δp_{ann} [bar]
1	19	0	1.06	1.77	0.439
2	-	-	-	2.82	0.694
3	-	-	-	3.90	0.955
4	-	-	-	4.92	1.20
5	-	-	-	6.00	1.38

Table 5.8: Configuration for spray angle favoured injector. This injector would be used when compromise between SMD and spray angle is necessary and spray angle is considered more critical.

Which results in the following performance.

Thrust level	SMD [μm]	α [degrees]	X [mm]
1	16.83	37.86	9.611
2	14.56	41.63	7.390
3	13.06	44.34	6.072
4	12.05	46.32	5.251
5	11.81	49.14	4.845

Table 5.9: Performance of spray angle favoured injector configuration. Due to the weighting spray angle values here are close to those in table 5.5, but slightly worse

This Injector configuration showcases a design where spray angle values are slightly favoured. Due to the higher spray angle weighting factor spray angle of table 5.9 will be close to those of table 5.5. But due to the fact that other performance parameters are also considered the spray angle values will be slightly worse than the injector where only spray angle is considered.

Injector 5: Balanced ($Q_D = 1$, $Q_\alpha = 1$, $Q_X = 1$)
In this injector no particular performance parameter is favoured over the others.

Thrust level	D_{pt} [mm]	θ_{pt} [degrees]	δ_{ann} [mm]	Δp_{pt} [bar]	Δp_{ann} [bar]
1	19	0	0.86	1.77	0.680
2	-	-	-	2.82	1.08
3	-	-	-	3.90	1.48
4	-	-	-	4.92	1.86
5	-	-	-	6.00	2.14

Table 5.10: Configuration for a balanced injector. This injector would be used when no particular performance parameter is favoured.

Which results in the following performance.

Thrust level	SMD [μm]	α [degrees]	X [mm]
1	12.64	34.56	6.692
2	10.63	38.14	4.869
3	9.333	40.74	3.828
4	8.463	42.66	3.196
5	8.161	45.42	2.854

Table 5.11: Performance of a balanced injector configuration. Due to the balanced weights this injector exhibits pretty average performance compared to other configurations.

This Injector configuration showcases a design where no performance parameter is favoured. Due to the balanced weighting factors the performance values of table 5.11 will be at an approximate middle ground for all parameters.

5.5 Final Injector

When selecting the final configuration is important to look at what factors are important to the project that the injector is being designed for. With the greatest weight factor placed on the performance parameters that are deemed most important. In this project there is no focus on a particular performance parameter which means the Q values should be relatively balanced. A slight weight is however put on SMD and vaporisation distance, because of their great impact on combustion performance.
Injector 6: Final choice ($Q_D = 2$, $Q_\alpha = 1$, $Q_X = 1.5$)

Thrust level	D_{pt} [mm]	θ_{pt} [degrees]	δ_{ann} [mm]	Δp_{pt} [bar]	Δp_{ann} [bar]
1	19	0	0.70	1.77	1.04
2	-	-	-	2.82	1.65
3	-	-	-	3.90	2.27
4	-	-	-	4.92	2.86
5	-	-	-	6.00	3.29

Table 5.12: Configuration of final injector. The configuration is represented visually in figure 5.10

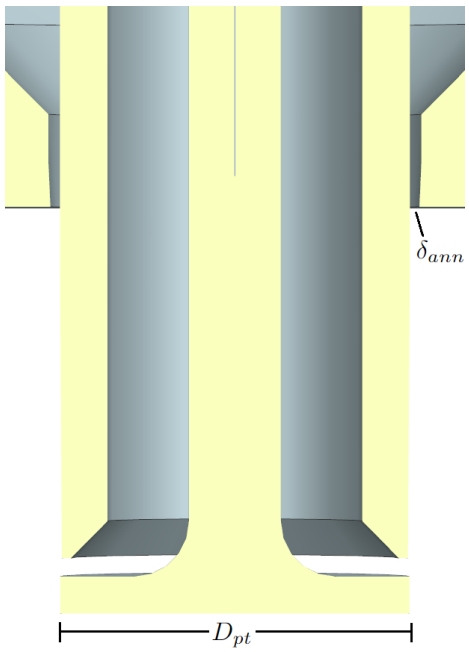

Figure 5.10: Graphic representation of final injector outlet region design.

Which results in the following performance.

Thrust level	SMD [μm]	α [degrees]	X [mm]
1	9.474	31.51	4.632
2	7.768	34.89	3.198
3	6.681	37.37	2.413
4	5.962	39.21	1.950
5	5.666	41.87	1.691

Table 5.13: Performance of final injector configuration. The results here show a slight favour towards better SMD and vaporisation distance, as designed by the Q values selected.

This injector configuration showcases great performance, the Q values selected have resulted in an injector with a slight focus on smaller SMD values. The spray angles and vaporisation distance values are however not neglected and they also showcase great performance. This injector configuration is deemed to be appropriate as a preliminary design which showcases that the design process can be considered a success.

CHAPTER 6

Discussion

6.1 Validating Performance

Table 5.13 shows the theoretical performance of the final injector chosen in the design process. Validating the results of SMD and vaporisation distance with simulations poses a challenge. Droplet generation and vaporisation are difficult to accurately model, especially so in a thrust chamber environment, validating these results are therefore deemed to be outside the scope of this thesis. Spray angles are however modelled by assuming that the effects of combustion and vaporisation can be ignored. Since the spray angle equation 3.17 is only dependant on TMR this assumption should still provide accurate results.

The following simulation results showcase the spray angle of thrust levels 2-5, the goal here is to verify the results from table 5.13. The simulations were performed in COMSOL Multiphysics.

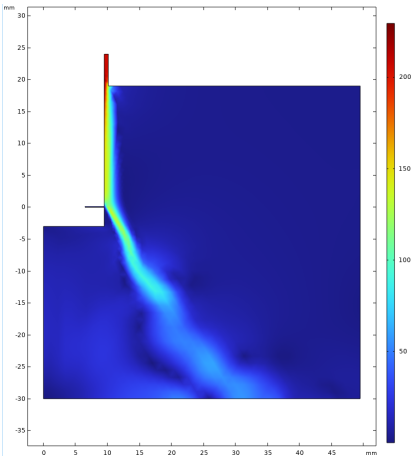

(a) Thrust level 2, desired spray angle: 34.9°

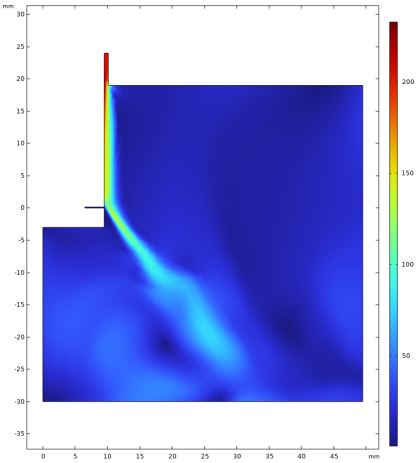

(b) Thrust level 3, desired spray angle: 37.4°

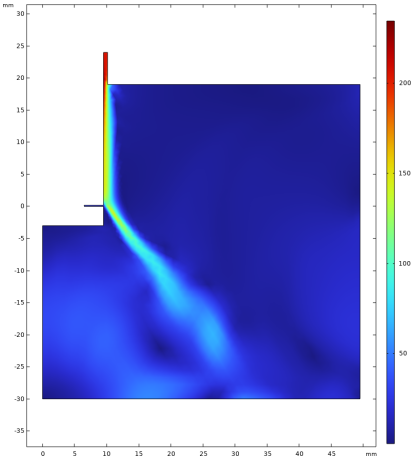

(c) Thrust level 4, desired spray angle: 39.2°

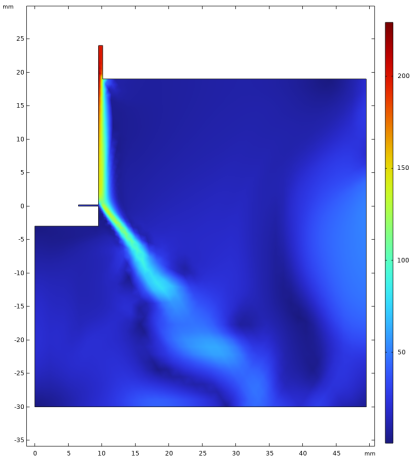

(d) Thrust level 5, desired spray angle: 41.9°

Figure 6.1: Spray angle simulation results. The Spray angle is acquired by measuring the angle between the velocity profile of the annular fluid and the y-axis.

The spray angle simulations in figure 6.1 show good correlation to the theoretical results of table 5.13. This indicates that the the calculated values are likely accurate.

6.2 Internal Geometry Design

Since the design process is focused on the outlet region the rest of the injector dimensions will be based on engineering experience and previous research. The main area of the injector that was neglected by the design process is the internal geometry of the injector.

The injector inlets will deliver the propellants to the injector through a simple tube. The internal geometry of the injector must be designed in such a way that the propellants will be uniformly distributed from a single flow source, this will be accomplished by designing a propellant manifold. In general a well designed manifold will contain few flow restrictions in order to distribute the propellants equally across the injector exit orifices, this dictates a large manifold volume. [6] In order to simplify the design of the injector the propellant inlets will inject the fluid radially to the injector. This means that the manifold being designed here must be able to convert the radial velocity into axial velocity. Previous research has shown that the annular flow is particularly difficult to distribute uniformly due to the tendency of the fluid to swirl around the injector sleeve and exit the annular orifice with some angular velocity. This effect can be mitigated by the using a distribution plate with holes that will redirect the angular flow into axial flow before it arrives at the annular orifice. The position, size and number of holes of the distribution plate is usually decided by engineering experience. In this project these holes are based on what previous injector designs used [30].

A few extra points were taken into consideration as the design was produced. Part count is kept to a minimum and most components are built as solids of revolution, this means they can be manufactured using ordinary industrial grade machining centres. The injector should be easy to assemble and disassemble, it is therefore designed in a way where each component is placed on the previous in a stack configuration. The top of the injector should also be free of obstacles in order for a pintle control mechanism to be attached. The skip distance (L_{skip} in figure 2.4) should be equal to the pintle diameter according to engineering experience [31].

With these design considerations and the variables calculated in the design process the following injector is designed in Siemens NX.

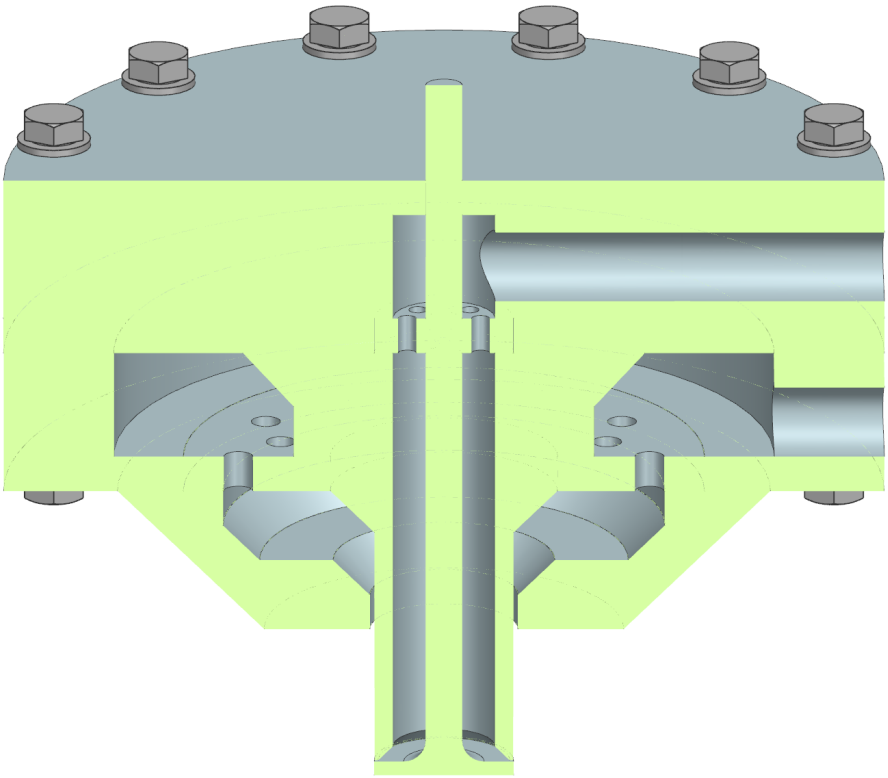

Figure 6.2: Cross section of the completed injector design. Notice the annular manifold design, it consists of a upper and lower torus shape, separated by a distribution plate.

Additional images of the model and sketches of the individual components can be found in appendix A.

In order to evaluate the quality of the internal geometry design a number of flow simulations are performed, these are visually evaluated here.

6.2.1 Outlet Flow Uniformity

The following simulations show the exit velocity magnitude of the the exit orifices. These Simulations were performed with Autodesk CFD 2023.

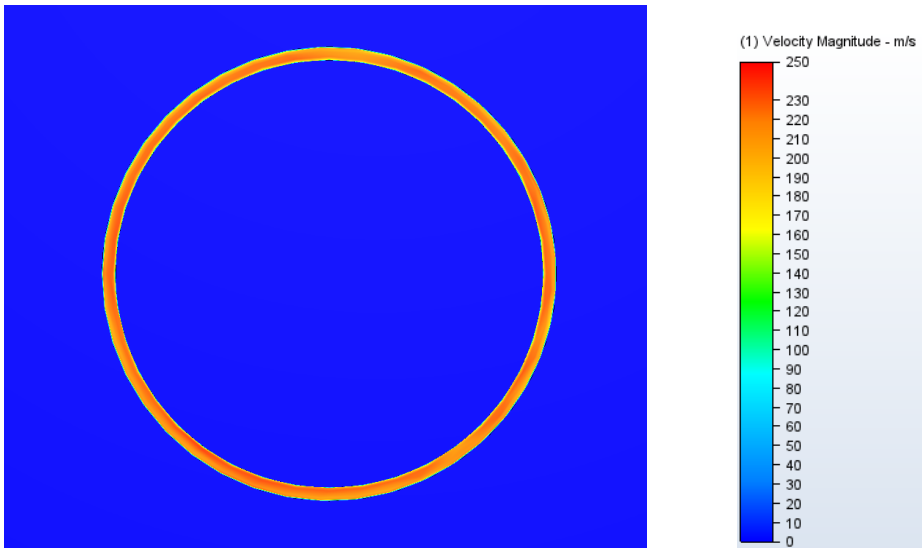

Figure 6.3: Propellant velocity out of the annular orifice. Uniformity in the velocity magnitude around the orifice indicates flow uniformity.

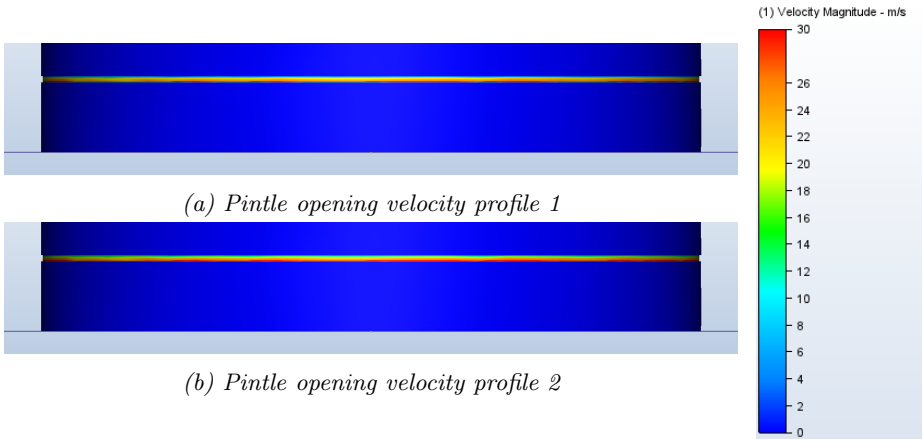

(a) Pintle opening velocity profile 1

(b) Pintle opening velocity profile 2

Figure 6.4: Propellant velocity out of the pintle, subfigures a and b show opposite sides of the pintle. Uniformity in the velocity magnitude around the orifice indicates flow uniformity.

Figures 6.3 and 6.4 show the velocity magnitude out of the exit orifices. Non-uniformity in this magnitude would indicate that the flow is uneven which in turn would result in an uneven spray. Through visual inspection of these two figures one can see that the velocity magnitude is well distributed in both images, there are no zones of excessively high or low velocities. This indicates that the

flow out of the injector will be uniform. These results should be supplemented by a real world test once the injector is complete but for a preliminary design study these results are promising.

6.2.2 Internal Flow

The following simulations show the streamlines of the fluid flow through the injector internals. These Simulations were performed using Autodesk CFD 2023.

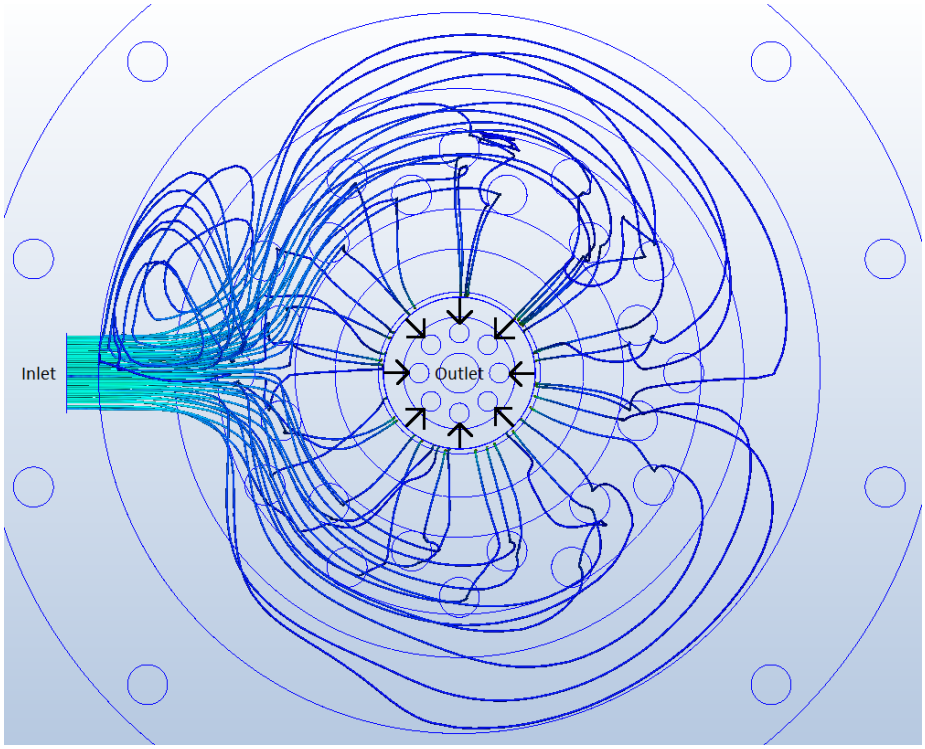

Figure 6.5: Streamlines of the annular propellant through the manifold, image taken from the top of the injector with the inlets oriented to the left. The streamlines illustrate the tendency of the propellant to swirl as it enters the manifold. It is desirable for the streamlines to be redirected towards the centre.

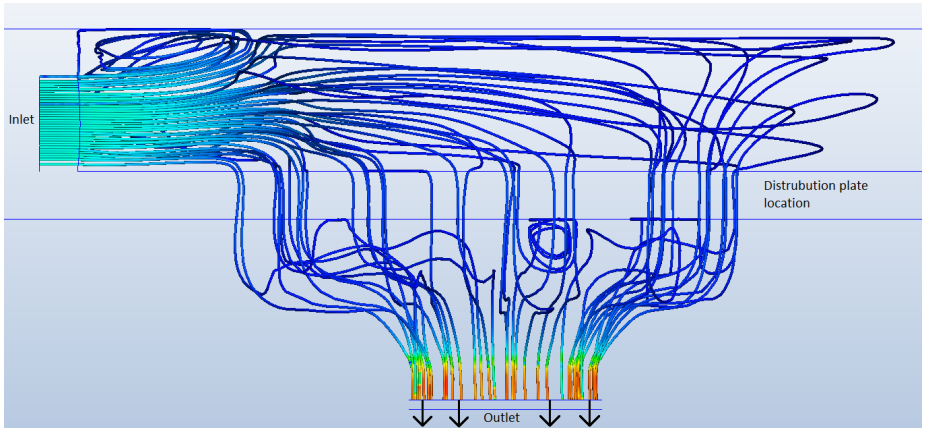

Figure 6.6: Streamlines of the annular propellant through the manifold, image taken from the side of the injector with the inlets oriented to the left. Propellant is injected from the left of the image and should be redirected straight down. The effects of the distribution plate are demonstrated as the fluid turns sharply into the lower manifold torus.

Figures 6.5 and 6.6 show the fuel flow though the manifold, the main aim here is to showcase how well the injector redirects the propellant from the inlet into the annular orifice. This is evaluated by visual observation of how well directed the streamlines are as they exit the injector at the centre of figure 6.5 and the bottom of Figure 6.6. Both images indicate a well designed manifold as the streamlines are properly redirected, these results should be supplemented by real world tests when possible.

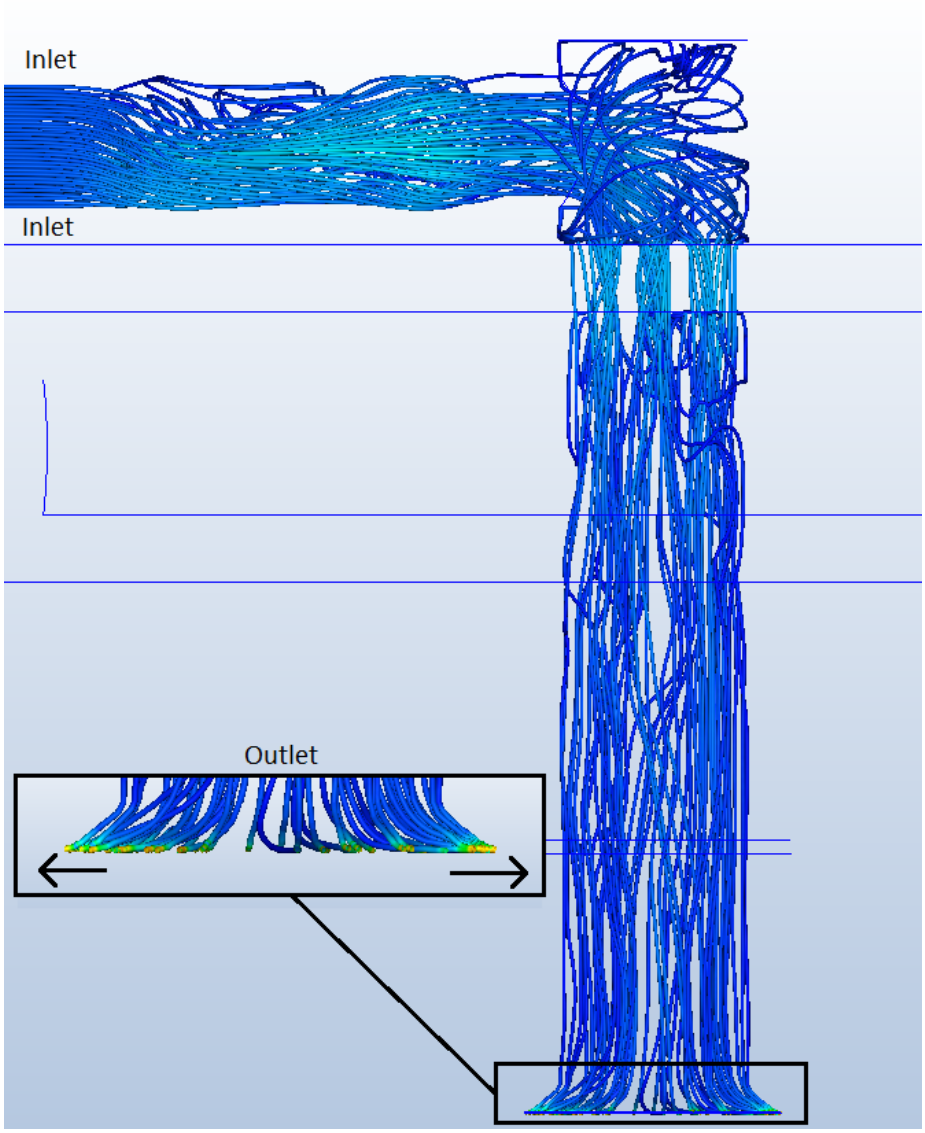

Figure 6.7: Streamlines of the pintle propellants through the injector, image taken from the side of the injector with the inlets oriented to the left. A close-up of the outlet region is included, with the desired flow direction.

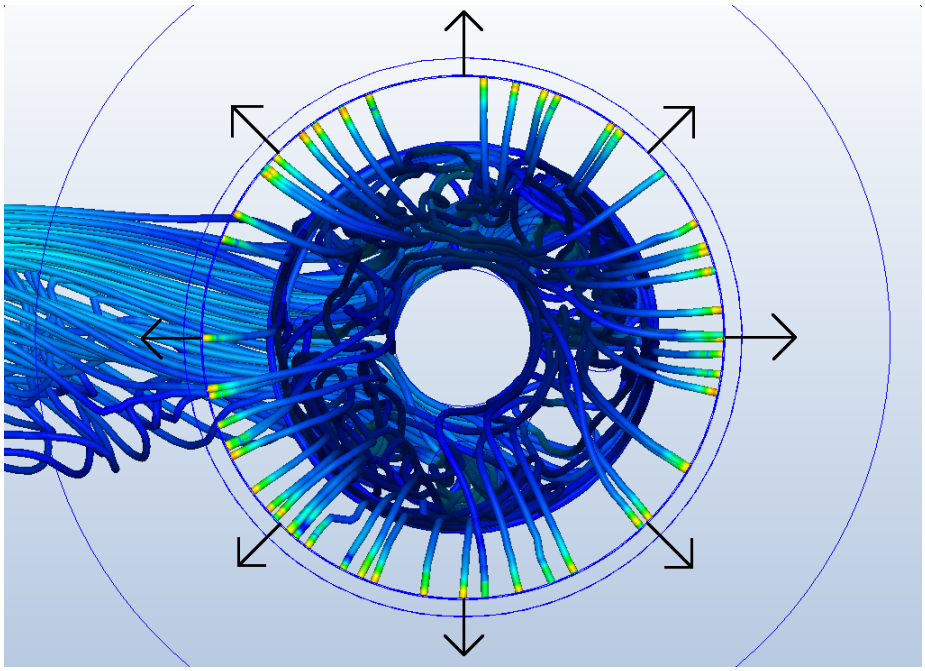

Figure 6.8: Streamlines of the pintle propellants through the injector, image taken from the bottom of the injector with the inlets oriented to the left. Propellant is injected from the left of the image and should be redirected radially from the centre of the image (in the direction of the arrows).

Figures 6.7 and 6.8 show the oxidiser flow though the injector, the main aim here is to showcase how well the injector redirects the propellant from the inlet into the pintle orifice. This is evaluated by visual observation of how well directed the streamlines are as they exit the injector at the centre of figure 6.8 and the bottom of Figure 6.7. Both images indicate a well designed manifold as the streamlines are properly redirected, these results should be supplemented by real world tests when possible.

6.3 Cold Flow Suggestions

The basic cold flow test should replace the LOX with water and the methane with air. This will change the fluid properties of both propellants, with the important parameters being density, viscosity and the surface tension of the liquid. And since the test will be conducted without a thrust chamber p_c will be equal to atmospheric pressure for all thrust levels.
An example of if the injector configuration from table 5.12 is used under cold test conditions with no change in mass flow rate is presented here. The pressure drop of the liquid is kept at the same level as for the actual injector but the

annular pressure drop must be changed in order to keep the same mass flow. The following performance is expected. (Vaporisation distance is not included since water wont vaporise in atmospheric conditions.)

Thrust level	SMD [μm]	α [degrees]	U_{gas} [m/s]	U_{liq} [m/s]
1	10.87	17.99	666.6	13.19
2	6.328	16.11	1058	16.65
3	4.111	14.91	1460	19.58
4	2.928	14.11	1839	21.99
5	2.252	13.88	2179	24.29

Table 6.1: Performance of final injector during cold flow test. U_{gas} is the velocity of the cold gas and U_{liq} is the velocity of the cold liquid.

These results present many difficulties for several reasons. The first, while smaller SMD are beneficial for the combustion process, smaller SMD in a cold flow test may increase the difficulty since the resolution demands on the measurement instrument will increase as the particles of interest decrease in size. α is much smaller than what is desired in a real injector, this is not of great concern since the angle can still be easily measured. The greatest problem comes from the velocity of the cold gas (U_{gas}), it is all supersonic and even hypersonic for higher thrust levels. This showcases that it is impossible to use the fuel mass flow rate during the cold flow test. The liquid velocity is of approximately the same magnitude as the hot firing parameters and doesn't present a problem.

The easiest way to solve this is by significantly decreasing the mass flow rate of the annular gas until its velocity is below sonic velocities. A gas velocity of $300 m/s$ is set as a goal and by using equations 3.4 and 3.9 a new gas mass flow is acquired, this gas flow will be constant for all thrust levels due to the atmospheric conditions. With this change the following results are expected during a cold flow test.

Thrust level	$\dot{m}_{gas}$ [kg/s]	Δp_{ann} [bar]	$\dot{m}_{liq}$ [kg/s]	Δp_{pt} [bar]
1	0.0140	0.847	0.0811	0.77
2	-	-	0.1288	2.82
3	-	-	0.1777	3.90
4	-	-	0.2238	4.92
5	-	-	0.2754	6.00

Table 6.2: Flow rates and pressure drops for the cold flow test.

Thrust level	SMD [μm]	α [degrees]	U_{gas} [m/s]	U_{liq} [m/s]
1	28.09	37.11	300	13.19
2	31.65	48.49	-	16.65
3	34.65	56.79	-	19.58
4	36.59	62.53	-	21.99
5	38.74	67.27	-	24.29

Table 6.3: Expected performance of final injector during cold flow test with modified flow rates.

By performing a cold flow test with the designed injector using the mass flow rates from table 6.2 the results from table 6.3 can be verified. If the cold flow test results show good correlation to the results of table 6.3 it would indicate that the expected performance in table 5.9 of the hot fired injector are likely to also be valid. This is due to the fact that the process of atomisation and spray generation are only slightly impacted by the propellant reaction [32].

6.4 Adaptability

The design process presented in this report can also easily be adapted for a variety of different conditions by changing the initial requirements or parameters. For instance by changing the propellant a new injector design can be produced by following the same steps taken in this report with the new propellant. The cost function can also easily be amended if a new performance parameter is identified by simply adding the new parameter to the state vector and a corresponding Q value in the weighting matrix. An example of this is shown in equation 6.1 where a generic performance parameter P has been added. When adding new parameters it is also important to find and add the necessary design variables of the generic performance parameter to the design algorithm aswell.

$$J = Q_{level} \begin{bmatrix} D_{32} \\ \alpha \\ X \\ P \end{bmatrix}^T \begin{bmatrix} Q_D & 0 & 0 & 0 \\ 0 & -Q_\alpha & 0 & 0 \\ 0 & 0 & Q_X & 0 \\ 0 & 0 & 0 & Q_P \end{bmatrix} \begin{bmatrix} D_{32} \\ \alpha \\ X \\ P \end{bmatrix} \tag{6.1}$$

This makes the process flexible and the design can easily be retuned with new values via the cost function.

CHAPTER 7

Conclusion

The purpose of this master thesis was to develop and demonstrate a method to design and optimise the outlet region of a pintle injector. This was accomplished by first investigating the primary challenges and advantages of the pintle injector, various parameters important to combustion performance were identified here. These parameters were then used in the design as optimisation goals. By using the numerical relationships of the performance parameters a set of design variables were identified, these variables were found to be in conflict during the optimisation process. This was solved through the use of a cost function, it was then shown that the optimal injector configuration for a specific application could be found by changing the Q values of the cost function. This meant that multiple outlet region designs could be constructed and evaluated rapidly. The design process presented in this report was also shown to be easily adapted for a variety of different conditions by changing the initial requirements or parameters.

An example of a specific pintle injector outlet design was then produced using the design method that was developed. This design was then evolved into a complete injector design and its performance was evaluated. The chosen injector was deemed to show great promise as a preliminary design.

In conclusion the design method produced in this thesis is deemed a success. It showed that a preliminary pintle injector design could be designed and optimised using a numerical approach. And once it has been manufactured cold flow testing can provide great research value by enabling a variety of studies on the characteristics of pintle injectors.

7.1 Future Work

Future work should be focused on two main goals, to finalise the design and to prepare for a cold flow test. In order for the design to be finalised the practical considerations of operating the injector should be investigated, this includes things like how to seal the propellant flow channels, how the injector shall be feed with cold flow propellants and how to manufacture it. Here a material study should also be conducted in order to find the best component material, a recommended starting point would be to investigate aluminium.
For the cold flow test there needs to be an investigation of which instruments are needed, developing general test procedures and how to construct the test rig. Extra care should be taken when designing this test rig, since the injector will spray water over an area it is imperative that sensitive instruments are kept safe from the spray without impacting the quality of the measurements.

Bibliography

[1] George P. Sutton and Oscar Biblarz. *Rocket Propulsion Elements, Eighth Edition*. 2010. ISBN: 9780470080245.

[2] K. Simhachalam Naidu M. Thirupathi N. Madhavi. "Design and Analysis of a Fuel Injector of a Liquid Rocket Engine". In: *International Journal of Engineering and Advanced Technology* 4.5 (2015), pp. 105–116. URL: https://www.ijeat.org/wp-content/uploads/papers/v4i5/E4105064515.pdf.

[3] Matthew J. Casiano, James R. Hulka, and Vigor Yang. "Liquid-Propellant Rocket Engine Throttling: A Comprehensive Review". In: *Journal of Propulsion and Power* 26.5 (2010), pp. 897–923. DOI: 10.2514/1.49791. eprint: https://doi.org/10.2514/1.49791. URL: https://doi.org/10.2514/1.49791.

[4] Joaquim Martins and Andrew Ning. *Engineering Design Optimization*. Oct. 2021. ISBN: 9781108833417. DOI: 10.1017/9781108980647.

[5] Phillip Hill and Carl Peterson. *Mechanics and Thermodynamics of Propulsion, Second Edition*. 1991. ISBN: 9780201146592.

[6] Dieter K. Huzel et al. *Modern engineering for design of liquid-propellant rocket engines / Dieter K. Huzel and David H. Huang ; revised, updated, and enlarged by Harry Arbit... (et al.)* English. American Institute of Aeronautics and Astronautics Washington, 1992. ISBN: 1563470136.

[7] Erin Betts and Robert Frederick. "A Historical Systems Study of Liquid Rocket Engine Throttling Capabilities". In: *46th AIAA/ASME/SAE/ASEE Joint Propulsion Conference & Exhibit*. DOI: 10.2514/6.2010-6541. eprint: https://arc.aiaa.org/doi/pdf/10.2514/6.2010-6541. URL: https://arc.aiaa.org/doi/abs/10.2514/6.2010-6541.

[8] Peng Cheng et al. "On the prediction of spray angle of liquid-liquid pintle injectors". In: *Acta Astronautica* 138 (2017). The Fifth International Conference on Tethers in Space, pp. 145–151. ISSN: 0094-5765. DOI: https://doi.org/10.1016/j.actaastro.2017.05.037. URL: https://www.sciencedirect.com/science/article/pii/S0094576517304782.

[9] Gordon Dressler and J. Bauer. "TRW pintle engine heritage and performance characteristics". In: *36th AIAA/ASME/SAE/ASEE Joint Propulsion Conference and Exhibit*. DOI: 10.2514/6.2000-3871. eprint: https://arc.aiaa.org/doi/pdf/10.2514/6.2000-3871. URL: https://arc.aiaa.org/doi/abs/10.2514/6.2000-3871.

[10] Timothy Smith, Mark Klem, and Kenneth Fisher. "Propulsion Risk Reduction Activities for Non-Toxic Cryogenic Propulsion". In: *AIAA SPACE 2010 Conference & Exposition*. DOI: 10.2514/6.2010-8680. eprint: https://arc.aiaa.org/doi/pdf/10.2514/6.2010-8680. URL: https://arc.aiaa.org/doi/abs/10.2514/6.2010-8680.

[11] Min Son. "Correlations Between Spray and Combustion Characteristics of a Movable Pintle Injector for Liquid Rocket Engines". PhD thesis. Korea Aerospace University, 2017.

[12] Subhashree S. Toshith S. Phutane Vedanth S. Saoor R. Rajendran Samiksha Prasad. "DESIGN AND OPTIMIZATION OF PINTLE INJECTOR FOR LIQUID ROCKET ENGINE". In: *International Journal of Engineering Applied Sciences and Technology* 5.1 (2020), pp. 151–159. ISSN: 2455-2143. URL: https://www.researchgate.net/publication/343544285_DESIGN_AND_OPTIMIZATION_OF_PINTLE_INJECTOR_FOR_LIQUID_ROCKET_ENGINE.

[13] Min Son et al. "Numerical study on the combustion characteristics of a fuel-centered pintle injector for methane rocket engines". In: *Acta Astronautica* 135 (2017), pp. 139–149. ISSN: 0094-5765. DOI: https://doi.org/10.1016/j.actaastro.2017.02.005. URL: https://www.sciencedirect.com/science/article/pii/S0094576516314035.

[14] M. Barrère and F.A. Williams. "Comparison of combustion instabilities found in various types of combustion chambers". In: *Symposium (International) on Combustion* 12.1 (1969), pp. 169–181. ISSN: 0082-0784. DOI: https://doi.org/10.1016/S0082-0784(69)80401-7. URL: https://www.sciencedirect.com/science/article/pii/S0082078469804017.

[15] Przemyslaw B. Kowalczuk and Jan Drzymala. "Physical meaning of the Sauter mean diameter of spherical particulate matter". In: *Particulate Science and Technology* 34.6 (2016), pp. 645–647. DOI: 10.1080/02726351.2015.1099582. eprint: https://doi.org/10.1080/02726351.2015.1099582. URL: https://doi.org/10.1080/02726351.2015.1099582.

[16] Rocco J. A. F. F. Iha K. Gonçalves R. F. B. Gottmann C. A. Alves W. F. "Liquid Rocket Propellants: Ethanol as Fuel". In: *Global Journal of Advanced Research* 2.1 (2016), pp. 109–119. ISSN: 2394-5788. URL: http://gjar.org/publishpaper/vol2issue1/d86r80.pdf.

[17] Todd Neill et al. "Practical uses of liquid methane in rocket engine applications". In: *Acta Astronautica* 65.5 (2009), pp. 696–705. ISSN: 0094-5765. DOI: https://doi.org/10.1016/j.actaastro.2009.01.052. URL: https://www.sciencedirect.com/science/article/pii/S0094576509000630.

[18] *Starship*. URL: https://www.spacex.com/vehicles/starship/.

[19] Kim Newton. *NASA tests methane engine components for next generation landers*. 2015. URL: https://www.nasa.gov/centers/marshall/news/releases/2015/nasa-tests-methane-powered-engine-components-for-next-generation-landers.html.

[20] Realff M.J. Sun W. et al. Kruyer N.S. "Designing the bioproduction of Martian rocket propellant via a biotechnology-enabled in situ resource utilization strategy". In: *Nature Communications* 12 (2021). DOI: https://doi.org/10.1038/s41467-021-26393-7. URL: https://www.nature.com/articles/s41467-021-26393-7.

[21] Shivanand R. Patil. "Cold flow testing of laboratory-scale hybrid rocket engine test apparatus." In: (May 2021). DOI: 10.32920/ryerson.14644389.v1. URL: https://rshare.library.ryerson.ca/articles/thesis/Cold_flow_testing_of_laboratory-scale_hybrid_rocket_engine_test_apparatus_/14644389.

[22] Keonwoong Lee Jaye Koo Kanmaniraja Radhakrishnan Min Son. "Effect of injection conditions on mixing performance of pintle injector for liquid rocket engines". In: *Acta Astronautica* 150 (2018), pp. 105–116. eprint: https://doi.org/10.1016/j.actaastro.2017.12.012. URL: https://doi.org/10.1016/j.actaastro.2017.12.012.

[23] Peter Corke. *Robotics, Vision and Control*. 2017. ISBN: 783319544120. DOI: 10.1007/978-3-319-54413-7.

[24] Brunno Vasques and Oskar Haidn. "Effect of Pintle Injector Element Geometry on Combustion in a Liquid Oxygen/Liquid Methane Rocket Engine". In: July 2017. DOI: 10.13009/EUCASS2017-88.

[25] Taouba Jouini and Anders Rantzer. "On Cost Design in Applications of Optimal Control". In: *IEEE Control Systems Letters* 6 (2022), pp. 452–457. DOI: 10.1109/LCSYS.2021.3079642.

[26] Bonnie J. McBride Sanford Gordon. *Computer Program for Calculation of Complex Chemical Equilibrium Compositions and Applications I. Analysis*. 1994. URL: https://ntrs.nasa.gov/citations/19950013764.

[27] Bonnie J. McBride Sanford Gordon. *Computer Program for Calculation of Complex Chemical Equilibrium Compositions and Applications II. User Manual and Program Description*. 1996. URL: https://ntrs.nasa.gov/citations/19960044559.

[28] Shaoping Quan and David P. Schmidt. "Direct numerical study of a liquid droplet impulsively accelerated by gaseous flow". In: *Physics of Fluids* 18.10 (2006), p. 102103. DOI: 10.1063/1.2363216. eprint: https://doi.org/10.1063/1.2363216. URL: https://doi.org/10.1063/1.2363216.

[29] Min Son et al. "Design Procedure of a Movable Pintle Injector for Liquid Rocket Engines". In: *Journal of Propulsion and Power* 33.4 (2017), pp. 858–869. DOI: 10.2514/1.B36301. eprint: https://doi.org/10.2514/1.B36301. URL: https://doi.org/10.2514/1.B36301.

[30] Rene Rezende, Vladia Perez, and Amílcar Pimenta. "Experiments with Pintle Injector Design and Development". In: July 2015. DOI: 10.2514/6.2015-3810.

[31] S.D. Heister and N. Ashgriz. *Handbook of Atomization and Sprays*. ISBN: 9781441972644.

[32] James Hulka Gregg Jones R. Jeremy Kenny Marlow D. Moser. "Cold Flow Testing for Liquid Propellant Rocket Injector Scaling and Throttling". In: *NASA* (2006). URL: https://ntrs.nasa.gov/api/citations/20060047749/downloads/20060047749.pdf.

Appendices

APPENDIX A

Models and Sketches

A.1 Models

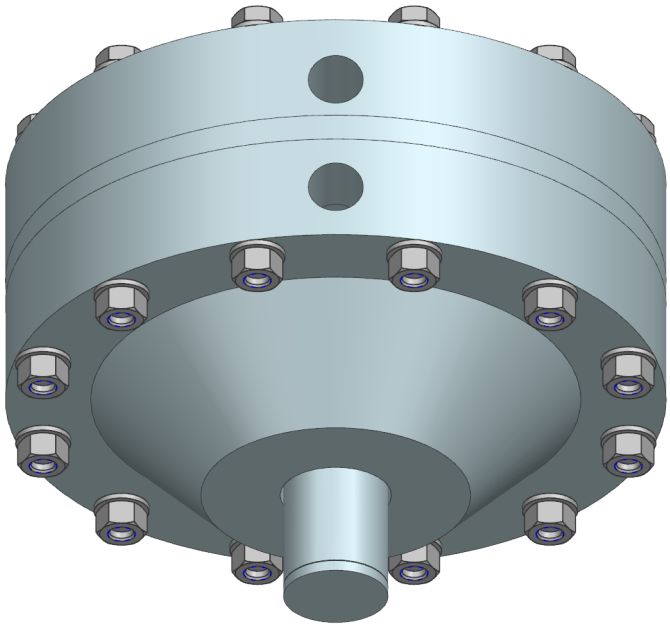

Figure A.1: Bottom view of the completed injector design. Bolts are hex head DIN M5x50.

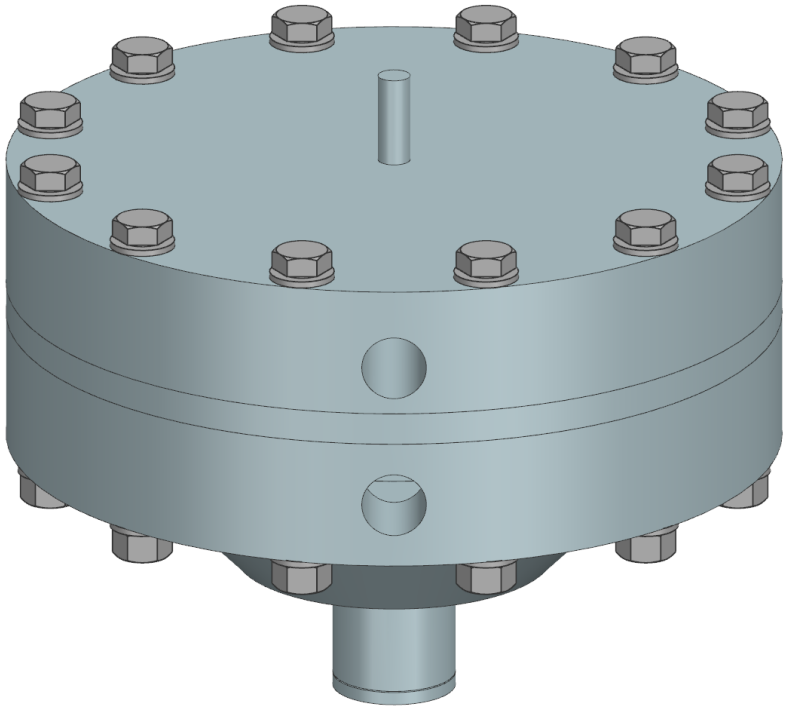

Figure A.2: Top view of the completed injector design. Bolts are hex head DIN M5x50.

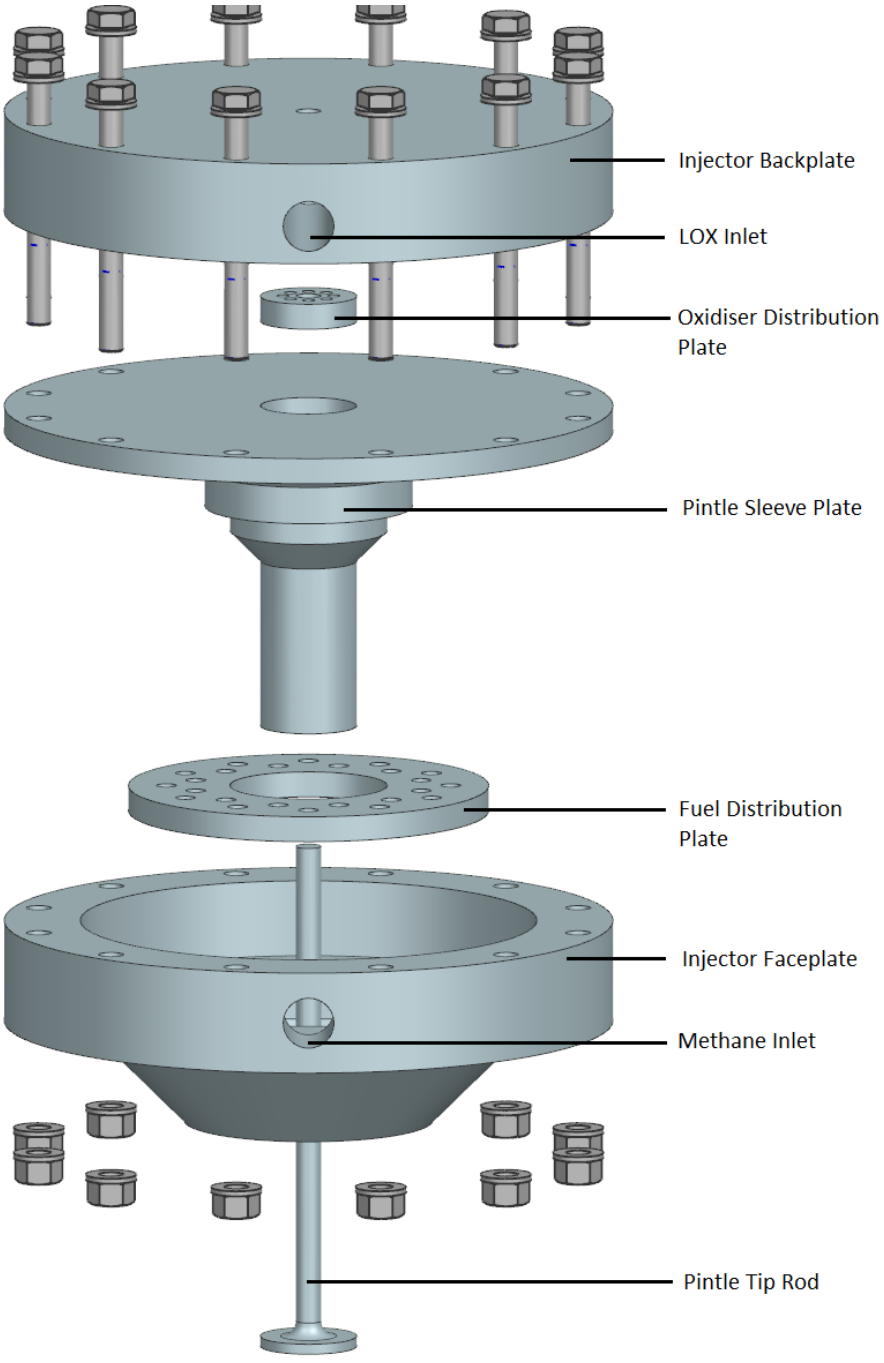

Figure A.3: Exploded view of the completed injector design with component names included.

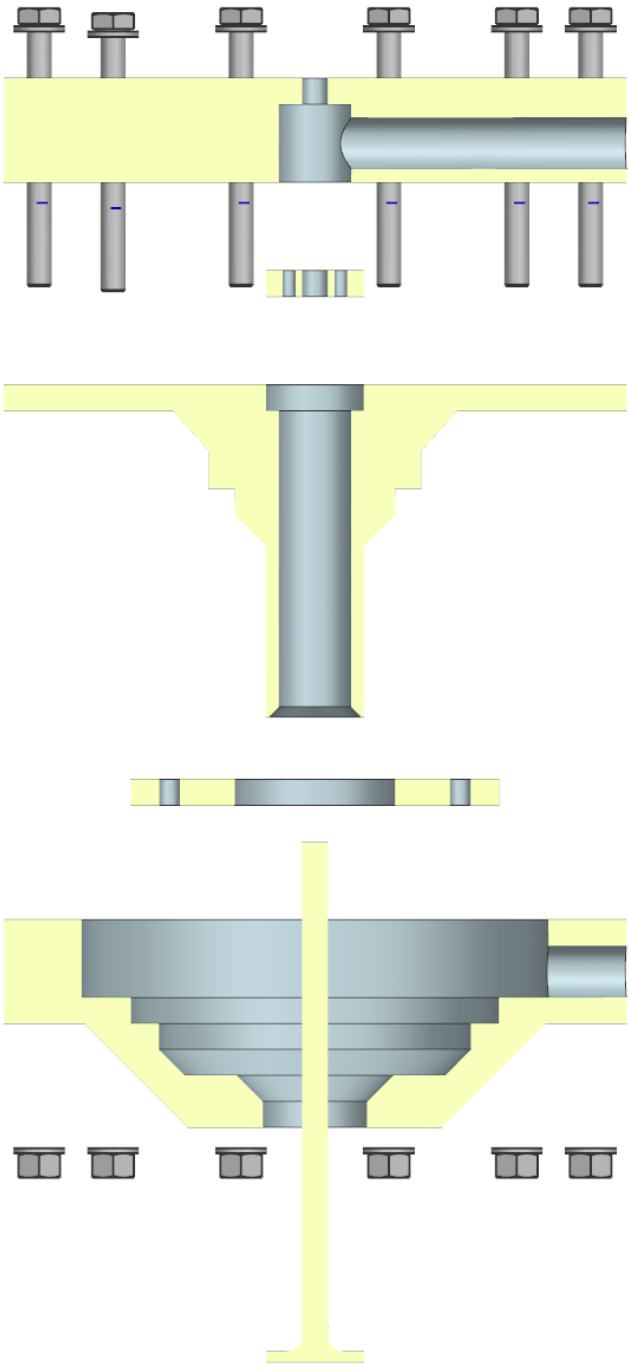

Figure A.4: Cross section of the exploded injector.

A.2 Sketches

Here sketches of the individual components from figure A.4 can be found. All measurements are in millimetres.

A.2.1 Backplate

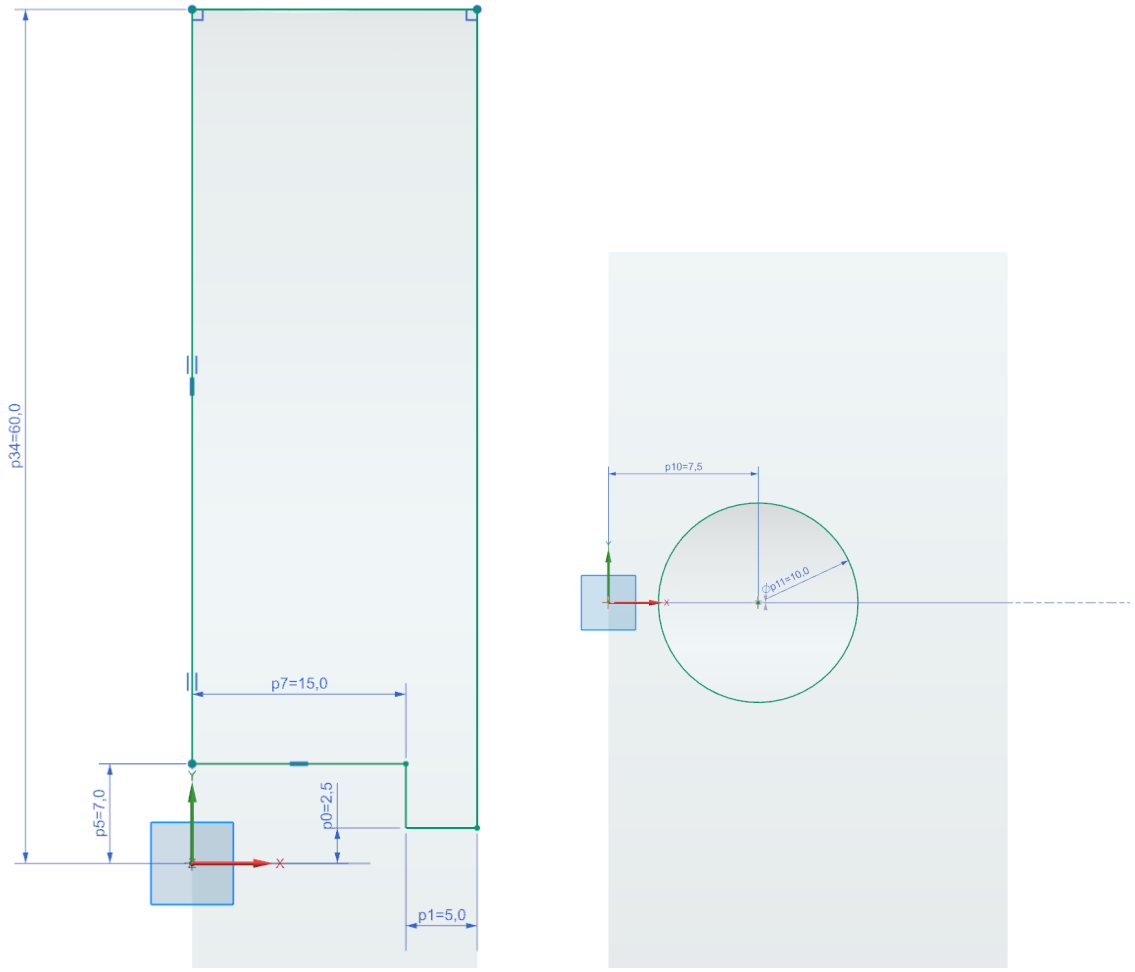

(a) Sketch of the backplate, finished component is axisymmetric around the horizontal x-axis.

(b) Oxidiser inlet size and position (Depth 60mm)

Figure A.5: Backplate sketches.

A.2.2 Oxidiser Distribution plate

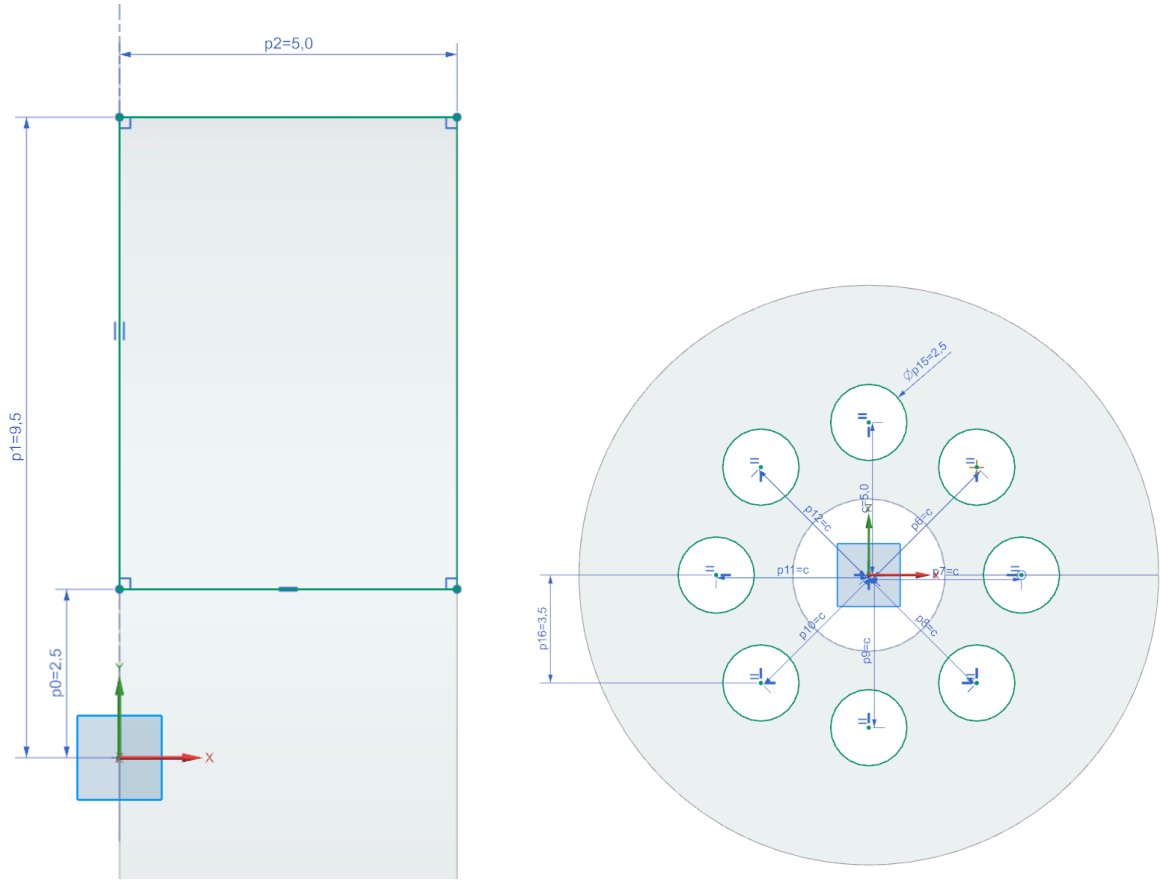

(a) Sketch of oxidiser distribution plate, finished component is axisymmetric around the horizontal x-axis.

(b) Size and position of oxidiser distribution plate holes.

Figure A.6: Oxidiser distribution plate sketches

A.2.3 Pintle Sleeve Plate

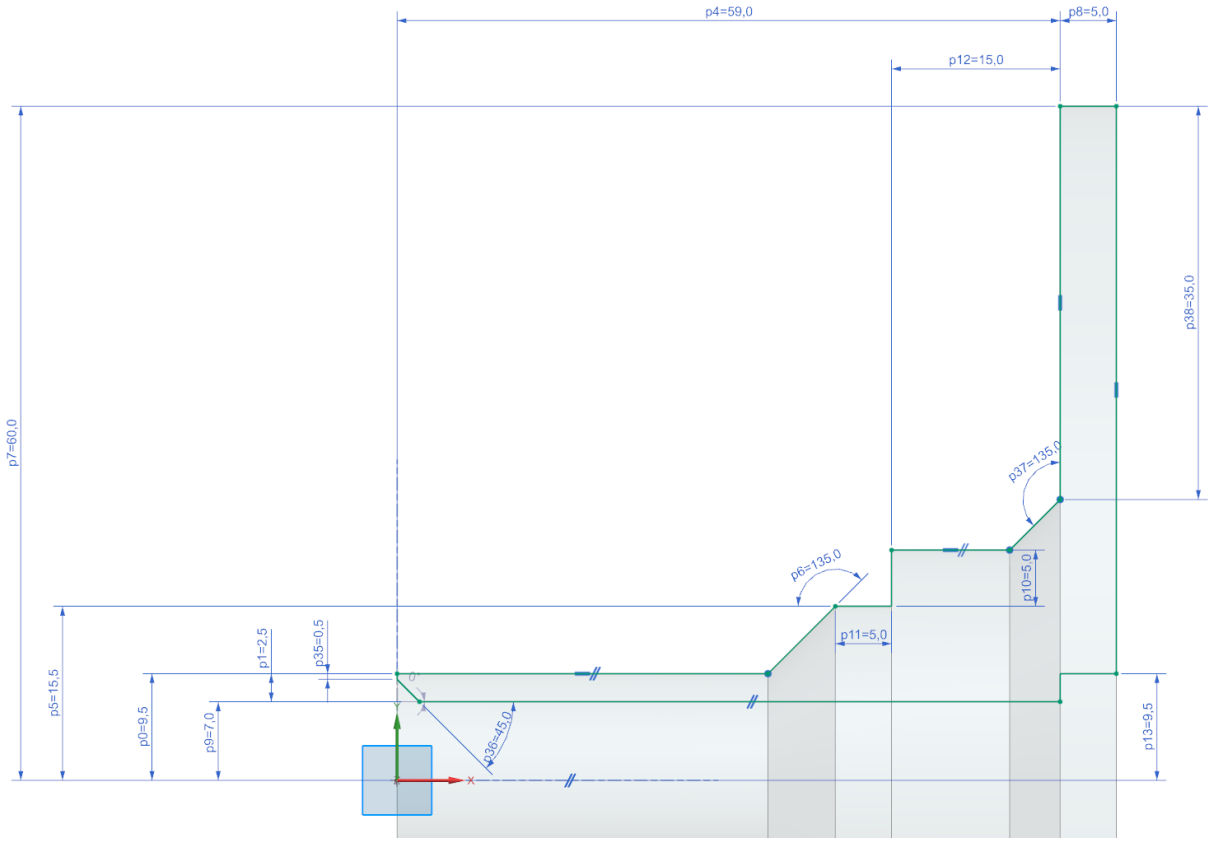

Figure A.7: Sketch of the pintle sleeve plate. Finished component is axisymmetric around the horizontal x-axis.

A.2.4 Fuel Distribution Plate

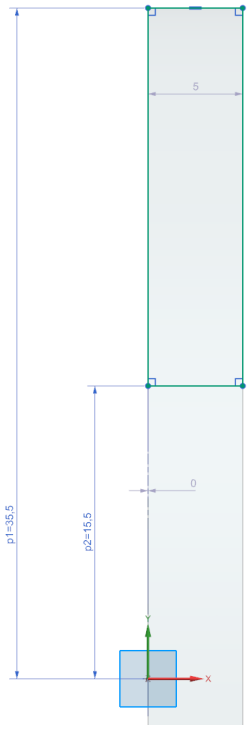

(a) Sketch of fuel distribution plate, finished component is axisymmetric around the horizontal x-axis.

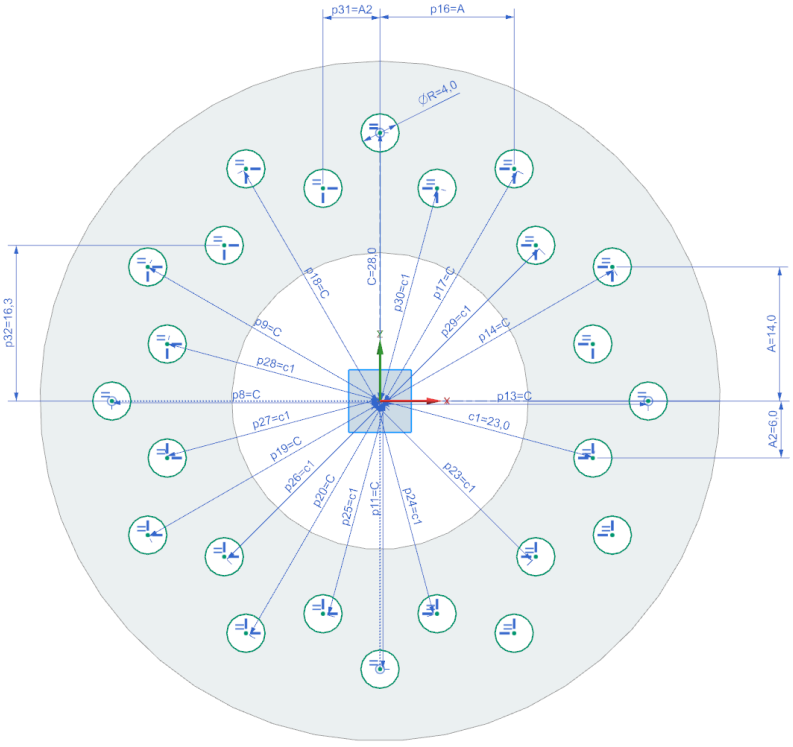

(b) Size and position of fuel distribution plate holes.

Figure A.8: Oxidiser distribution plate sketches

A.2.5 Injector Faceplate

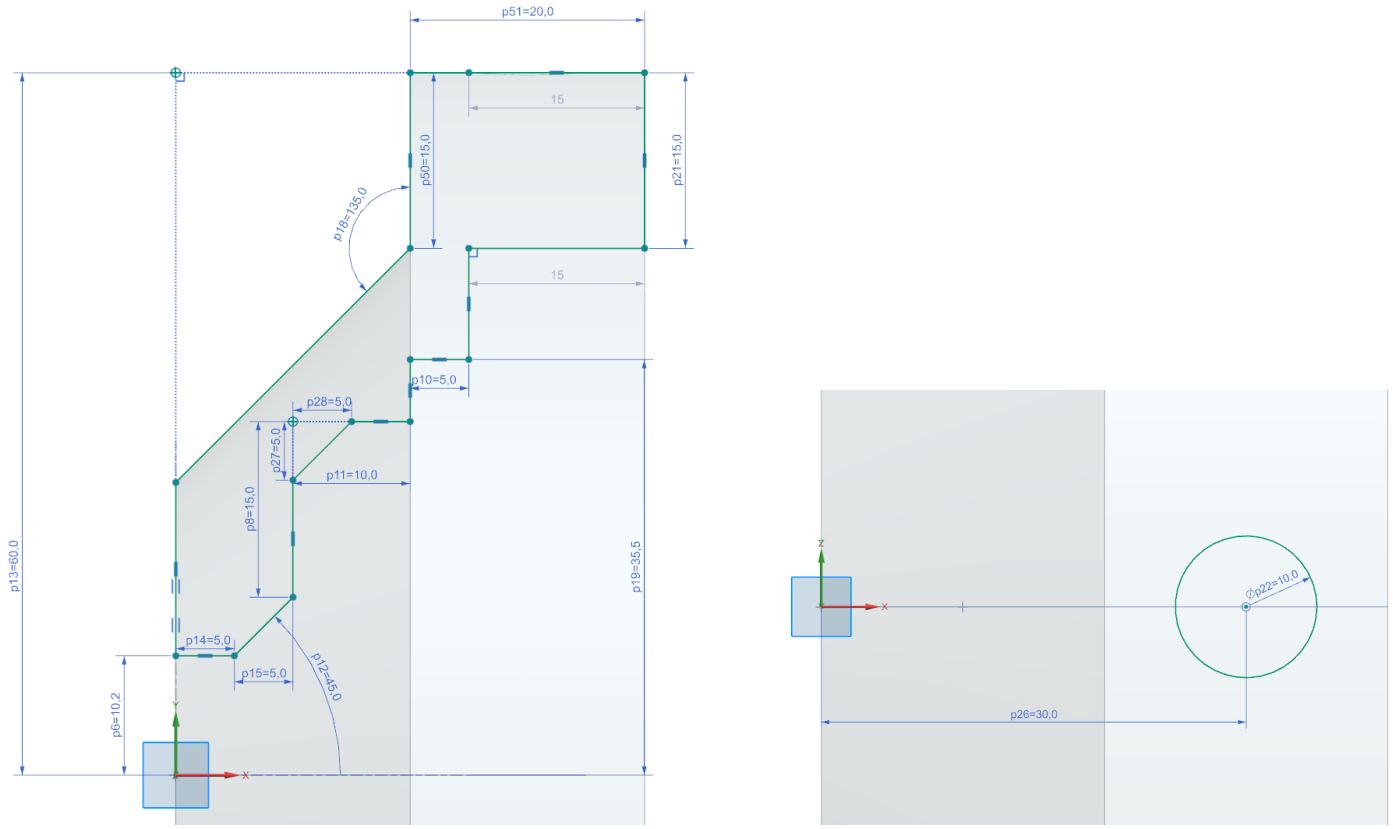

(a) Sketch of the faceplate, finished component is axisymmetric around the horizontal x-axis.

(b) Fuel inlet size and position (Depth 60mm)

Figure A.9: Faceplate sketches.

A.2.6 Pintle Tip Rod

Figure A.10: Sketch of the pintle sleeve plate. Finished component is axisymmetric around the horizontal x-axis.